The Spatial and Temporal Evolution of the Portland and Tualatin Basins, Oregon, USA

by

Darby Patrick Scanlon

A thesis submitted in partial fulfillment of the
requirements for the degree of

Master of Science
in
Geology

Thesis Committee:
John Bershaw, Chair
Ashley R. Streig
Ray E. Wells

Portland State University
2019

ABSTRACT

The Portland and Tualatin basins are part of the Puget-Willamette Lowland in the Cascadia forearc of Oregon and Washington. The Coast Range to the west has undergone Paleogene transtension and Neogene transpression, which is reflected in basin stratigraphy. To better understand the tectonic evolution of the region, I modeled three key stratigraphic horizons and their associated depocenters (areas of maximum sediment accumulation) through space and time using well log, seismic, outcrop, aeromagnetic, and gravity data. Three isochore maps were created to constrain the location of Portland and Tualatin basin depocenters during 1) Pleistocene to mid-Miocene (0-15 Ma), 2) eruption of the Columbia River Basalt Group (CRBG, 15.5-16.5 Ma), and 3) Mid-Miocene to late Eocene time (~17-35 Ma). Results show that the two basins each have distinct mid-Miocene to Pleistocene depocenters. The depth to CRBG in the Portland basin reaches a maximum of ~1,640 ft, 160 ft deeper than the Tualatin basin. Although the Portland basin is separated from the Tualatin basin by the Portland Hills, inversion of gravity data suggests that the two were connected as one continuous basin prior to CRBG deposition. Local thickening of CRBG flows over a gravity low coincident with the Portland Hills suggests that Neogene transpression in the forearc reactivated the Sylvan-Oatfield and Portland Hills faults as high angle reverse faults. This structural inversion separated the once continuous Portland and Tualatin basins in the mid-late Miocene. A change in the stress regime at that time marks the transition from Paleogene forearc extension to deformation dominated by north-south shortening due to collision of the forearc against the Canadian Coast Mountains. An eastward shift of the forearc basin

depocenter over the Neogene likely reflects uplift of the Coast Range to the west. A change in regional stress in the mid to late-Miocene, along with uplift of the Oregon Coast Range, caused a 10-fold decrease in sediment accumulation rates across the Portland and Tualatin basins. Transpressional oblique-slip faulting continues to deform the region as the forearc undergoes clockwise rotation and collides with the rigid Canadian Coast Mountains to the north.

ACKNOWLEDGEMENTS

This research wasn't done in isolation. Its fruition is the product of collaboration with the individuals listed below.

I would first like to thank my adviser, Dr. John Bershaw, for teaching me to think critically about my research and its implications. I'd also like to thank my committee members Drs. Ashely Streig and Ray Wells for their valuable insight and commitment to my success. I've definitely grown as a geologist during my time at Portland State University, and I've no doubt each of you have contributed to that. Thank you to Erick Burns from the U.S. Geological Survey for his helpful insight into the geologic modeling process, workflows, and professional report writing. I'd also like to thank Rick Blakely from the U.S. Geological Survey for providing me with the gravity inversion grid of McPhee et al., 2014. I can say that I've learned a great deal over the past few years, and I'm excited to apply that knowledge in the workforce.

Last, but certainly not least, special thank you to my parents and their continued support throughout this process. I wouldn't be where I am without your encouragement and enthusiasm for my chosen field. I look forward to sharing the wonders of geology with you both in the coming years!

Educational software licenses were provided by Esri™ and IHS Markit® for ArcGIS and Kingdom™, respectively. This research was supported by the Department of Energy's Office of Energy Efficiency and Renewable Energy (EERE) office through the Portland Deep Direct-Use Thermal Energy Storage (DDU-TES) Feasibility Study, Grant # DE-EE0008104.

TABLE OF CONTENTS

LIST OF FIGURES

CONVERSION FACTORS, DATUMS, ABBREVIATIONS, AND ACRONYMS

Conversion Factors

Multiply	By	To obtain
foot (ft)	0.3048	meter (m)
mile (mi)	1.609	kilometer (km)
square mile (mi^2)	2.590	square kilometer (km^2)

Datums

Vertical coordinate information referenced to the North American Vertical Datum of 1988 (NAVD88).

Horizontal coordinate information referenced to the North American Datum of 1983, Zone 10 (NAD83 Zone 10).

Elevation refers to distance in feet above (or below) NAVD88.

Measured depth refers to distance in feet below surface elevation.

Abbreviations and Acronyms

CRBG – Columbia River Basalt Group

DEM – Digital Elevation Model

DOGAMI – Department of Geology and Mineral Industries

GIS – Geographic Information System

GWIS – Groundwater Information System

NAM – North America

NWB – Northern Willamette basin

OWRD – Oregon Water Resources Department

PB – Portland basin

TB – Tualatin basin

TWT – Two-way travel time

USGS – United States Geological Survey

CHAPTER 1: INTRODUCTION AND GEOLOGIC SETTING OF THE PORTLAND AND TUALATIN BASINS

1.1 Introduction

The Portland and Tualatin basins are part of the Puget-Willamette Lowland, a forearc trough of the Cascadia subduction zone, formed by oblique convergence of the Juan de Fuca plate beneath North America (Evarts et al., 2009) (Figure 1.1). The Coast Range to the west has undergone Paleogene transtension and Neogene transpression, suggesting the basins have a complex history (Snavely and Wagner, 1963; Snavely et al., 1993; Snavely and Wells, 1996; McPhee et al., 2014). This change in stress regimes marks the transition from Paleogene forearc magmatism associated with extension to deformation dominated by north-south shortening due to collision of the forearc against the Canadian Coast Mountains (Wells and McCaffrey, 2013; Wells et al., 2014). Tracking basin depocenters (areas of maximum sediment accumulation) through space and time provides crucial constraints on the structural and tectonic evolution of the Cascadia forearc, as has been done in other basin analysis studies (Ingersoll, 1978; Zak and Freund, 1981; Heller et al., 1988; Flemings and Jordan, 1990). Prior workers suggest that the Portland basin formed under both transtensional and transpressional (Beeson et al., 1989a; Evarts et al., 2009) stress regimes, and that the Tualatin basin formed as a transtensional rhombochasm before mid-Miocene time (McPhee et al., 2014).

Previous studies integrating geological and geophysical data have been conducted in the Tualatin basin (Popowski, 1996; Wilson, 1997; McPhee et al., 2014) and in part of the Portland basin (Roe and Madin, 2013), though an integrated geologic model of both basins currently does not exist. Here, I synthesize well log, outcrop, seismic, aeromagnetic, and gravity data to better understand the stratigraphic architecture and role of these two basins in the active deformation of the Cascadia forearc.

Though no recent earthquakes larger than magnitude 6 (M 6) have occurred in the Willamette Valley, the region is seismically active (Yelin and Patton, 1991; Wong et al., 2001). Historic activity along individual faults is not well understood, leading to poor hazard prediction. Integrating Portland and Tualatin basin history into our understanding of forearc evolution provides a foundation for ongoing seismic hazard research in the Portland metropolitan and surrounding areas (Givler et al., 2009; Roe and Madin, 2013). Data derived from basin evolution studies includes cumulative fault displacement and slip rates through time, and is used in seismic hazard evaluations (Wong et al., 2000, 2001). My isochore maps show significant local thickening over a gravity low coincident with the Portland Hills, suggesting that the Sylvan-Oatfield and Portland Hills faults have been active since the Paleogene, and that the Portland Hills uplift is the product of Neogene structural inversion.

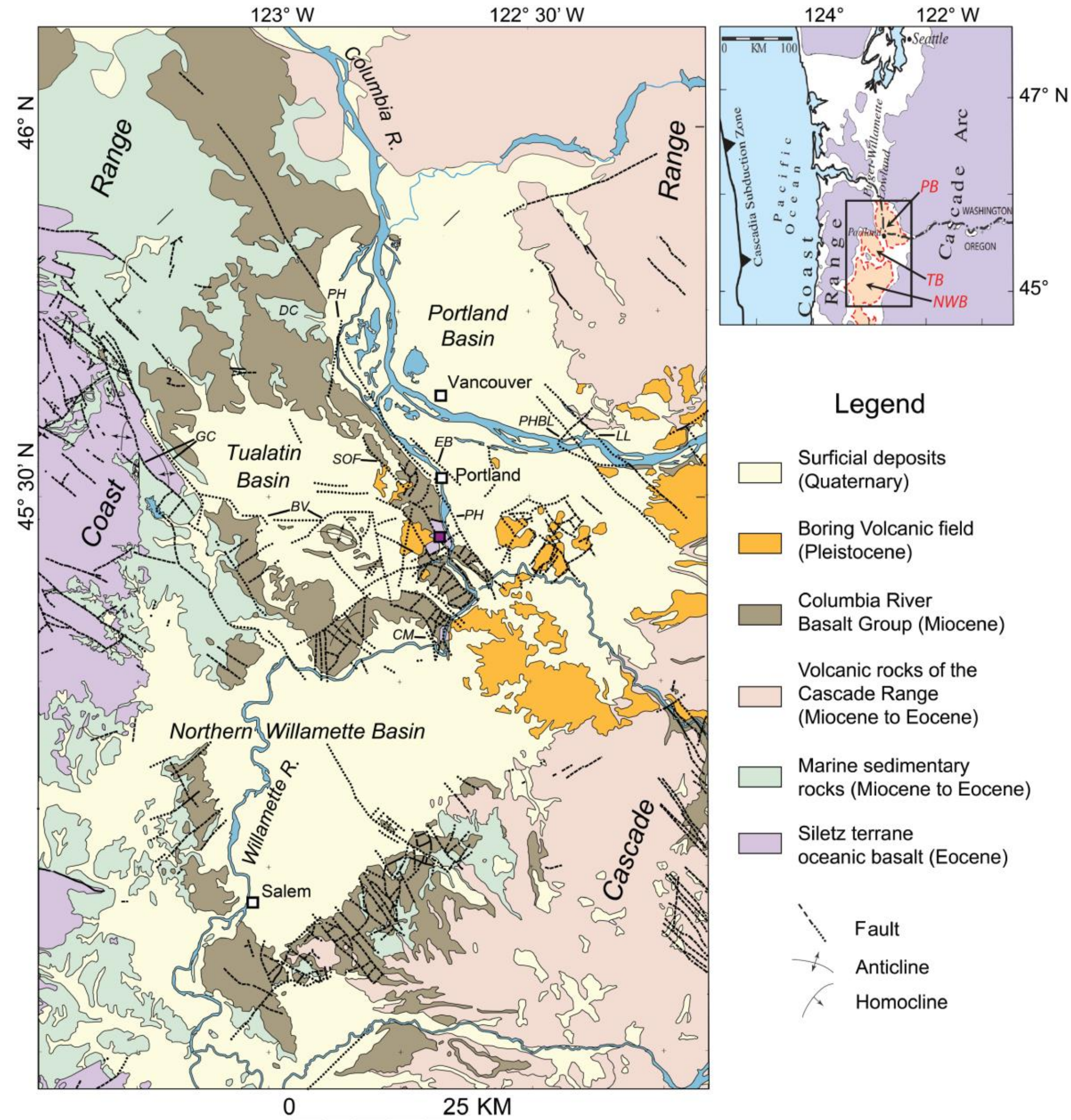

Figure 1.1. Generalized geology of the Portland and Tualatin basins, adapted from Blakely et al., 2000; McPhee et al., 2014 after Walker and MacLeod, 1991; Wells et al., 1994. GC – Gales Creek fault; BV – Beaverton fault; SOF – Sylvan-Oatfield fault; CM – Canby Molalla fault; PH – Portland Hills fault; EB – East Bank fault; PHBL – Prune Hill/Blue Lake fault; LL – Lacamas Lake fault; DC – Dutch canyon. White squares indicate major cities; Purple square indicates location of Eocene Waverly Heights basalt. Inset: PB – Portland basin; TB – Tualatin basin; - NWB – Northern Willamette basin.

1.2 Geologic Setting of the Portland and Tualatin Basins

Oblique subduction of the Juan de Fuca plate beneath North America has produced the Cascade Volcanic arc and tectonically active forearc (Wells et al., 1998). The Portland and Tualatin basins cover an area of approximately 3,885 km^2 and are part of the Puget-Willamette Lowland, a forearc trough situated between the Coast Range and western Cascades (Evarts et al., 2009; Bassett and Watts, 2015) (Figure 1.1). There is evidence of extension and shortening in both basins (Evarts et al., 2009; McPhee et al., 2014), however, the spatial and temporal distribution of deformation remains poorly understood (Blakely et al., 2000). Numerous northwest striking dextral strike-slip faults exist in the Portland and Tualatin basins (Blakely et al., 1995, 2004; Wong et al., 2001; Liberty et al., 2003; Evarts et al., 2009; Walsh et al., 2011; Wells et al., 2018). Previous workers suggest that the Portland basin may have formed as a pull-apart basin in response to the transfer of strain between the Portland Hills-Clackamas River structural zone and the Sandy River-Frontal fault zone (Beeson et al., 1985; Yelin and Patton, 1991), and that the Tualatin basin formed as a pull-apart basin bounded on the southwest by the Gales Creek fault (McPhee et al., 2014).

The stratigraphy of the Portland and Tualatin basins records a history of volcanism and sedimentation in both fluvial and marine depositional environments (Figure 1.2). Oceanic basalts and basaltic sedimentary rocks of the Siletz River Volcanics, commonly referred to as Siletzia, forms the Eocene basement underlying Cenozoic basin fill of the Willamette Valley (Snavely et al., 1968; Duncan, 1982; Yeats et al., 1996). Accretion of the Siletzia terrain to North America (NAM) at the latitude of Oregon occurred between 51-49 Ma (Wells et al., 2014). The southern part of the

Portland Hills uplift separating the two basins is underlain by the Eocene basalt of Waverly Heights, best exposed adjacent to the Willamette River near the Waverly Heights area (Beeson et al., 1989b; Blakely et al., 2004). West of the study area along the east flank of the Coast Range anticline, basement rocks are exposed as lower Eocene submarine basalt of the Siletz River Volcanics, associated diabase sills, and subaerial basalt of the mid-Eocene Tillamook Volcanics (Figure 1.1) (Trehu et al., 1994; Wells et al., 1994, 2014; Blakely et al., 2000). Miocene-Eocene flows of the western Cascade Volcanic arc erupted onto the accreted surface of Siletzia terrane, forming a constructional volcanic edifice on the eastern margin of the Portland basin (Beeson et al., 1989a). Faults and folds began to develop in the Eocene accompanying accretion of Siletzia and the onset of clockwise rotation of the forearc (Yeats et al., 1991, 1996; McCaffrey et al., 2007; Wells and McCaffrey, 2013).

Following the accretion of Siletzia to Oregon, both marine and marginal-marine sedimentary rocks were deposited in both basins during late Eocene and early Oligocene time. In the Portland basin, deposition of these sediments are coeval with eruptions from an incipient western Cascade Volcanic arc and their eastern edge mark the Paleogene coast (Evarts et al., 2010). Paleogene strata dipping basinward along the modern margins of the Portland basin indicate that a broad syncline began to form after ~20 Ma (Evarts, 2004a, 2004b, 2004c, 2006; Evarts et al., 2009b). Rogers (2002) suggests that phase changes in the down-dip direction of the subducting slab may have caused forearc subsidence. Previous workers suggest that the syncline formed coeval with uplift of Paleogene strata to form the Coast Range forearc high (Snavely and Wells, 1996; Evarts et al., 2009b). During the mid-Miocene, the Columbia River Basalt Group (CRBG) erupted from a series of dike swarms near the present day junction between Oregon, Washington, and Idaho (Tolan et al., 2009). At 15.5-16.5 Ma, voluminous flows of the Grande Ronde Basalt passed through the Cascade Range via the ancestral Columbia River into the nascent Portland and Tualatin basins (Beeson et al., 1989a; Beeson and Tolan, 1990). A decrease in Cascadian volcanism prior to CRBG emplacement meant that advancing flows may have encountered a relatively obstacle free path through the Cascade Range before inundating the basins (Hammond, 1979; Beeson et al., 1989a).

The stratigraphic architecture of the CRBG is poorly constrained on the eastern margin of the Portland basin, where the CRBG uncomformably overlies volcanic rocks of the western Cascades (Wells et al., 2018). Elevation maps and interpretive cross sections of CRBG and older rocks in the Portland basin show that depth to top CRBG is > 487 m towards the center of the basin along the Columbia River (Swanson et al., 1993). The modern boundaries of the Portland and Tualatin basins were established by the mid-Miocene based on distribution maps of the CRBG and gravity inversion (Beeson et al., 1989a; Evarts et al., 2009; McPhee et al., 2014). Previous workers suggest that the earliest flows of the CRBG were diverted by a nascent Portland Hills anticline and that later flows overcame this topographic barrier, also in the mid-Miocene (Beeson et al., 1989a; Evarts et al., 2009). See Figure A1 in the Appendix for a detailed stratigraphic column of the CRBG from Beeson et al. (1989a).

Interpretive cross sections based on a gravity survey through a light-rail tunnel (Blakely et al., 2004) in the Portland Hills show step like anomalies that are consistent with steeply dipping reverse faults bounding the Portland Hills anticline, and the authors note that there may exist a significant component of strike-slip displacement on the

Sylvan-Oatfield fault. Walsh et al. (2011) estimate modest shortening due to folding since CRBG emplacement. The Sylvan-Oatfield and Portland Hills faults comprise part of the larger Portland-Hills Clackamas River Structural zone described by Beeson et al. (1985, 1989a) and Blakely et al. (1995), which has experienced folding and faulting since mid-Miocene time (Figure 1.2) (Beeson et al., 1985; Blakely et al., 2004).

Post CRBG stratigraphy starts with the Rhododendron Formation, a volcanic mudflow breccia that overlies the CRBG on the southeast portion of the Portland basin, which was deposited in late Miocene time on the west flank of the Cascade Range (Trimble, 1963). The lower Sandy River Mudstone was deposited in the basin during the last half of the Miocene (Evarts et al., 2009). This unit is interpreted as lacustrine, consisting of silt and very fine sand (Trimble, 1963). At the end of the Miocene, the Columbia River began to deposit coarse sandstone and conglomerates of the lower Troutdale Formation. Clast composition suggests an extrabasinal source in pre-Cenozoic rocks in eastern Washington and Idaho (Evarts et al., 2009). The upper Sandy River Mudstone was also deposited during this time, suggesting the ancestral Columbia River was a meandering system with low energy floodplains (Tolan and Beeson, 1984; Evarts et al., 2009). Low potassium tholeiite (LKT) flows erupted at 3.5 Ma in the Cascade Range to the east, generating hyaloclasite as the LKT flowed into the ancestral Columbia River. This resulted in deposition of a hyaloclastic sandstone member of the Troutdale Formation, deposited as a volcaniclastic alluvial fan in the eastern portion of the Portland basin (Evarts et al., 2009). Overlying the CRBG in the Tualatin basin are ~450 m of unlithified to poorly lithified quartzo-micaceous sediments ranging in age from late Miocene to Pleistocene (Popowski, 1996). On the basis of gross lithology and stratigraphic position, Madin (1990) considered these sediments equivalent to the Sandy River Mudstone. However, Wilson and Peterson (1996) suggest that the Portland and Tualatin basins have been relatively isolated from each other since the late Miocene. Results from their analyses do not show Cascadian fluvial influence, suggesting a Coast Range source for post-CRBG sediments in the Tualatin basin (Popowski, 1996).

The present day topography of the Portland and Tualatin basins is influenced by geologic events of the past ~2.5 Ma. The Boring Volcanic field, consisting of cinder cones and associated lava flows, small shields, and lava cones, erupted west of the Cascade arc axis during the latest Pliocene (Treasher, 1942; Conrey et al., 1996; Evarts et al., 2009, 2010). This relatively young volcanic field exists in both the Portland and Tualatin basins, and is identified as high relief hills on the modern landscape. Quaternary terrace gravel deposits flanking the modern Columbia River resemble Troutdale Formation conglomerates, but contain a higher proportion of clasts derived from the Cascade Range (Evarts et al., 2009b). The volcaniclastic Springwater Formation consists of cobble gravel and mudflow deposits and flanks the Sandy and Clackamas rivers along the east and southeast margins of the Portland basin (Trimble, 1963; Evarts et al., 2009). More recently, late Pleistocene glacial outburst floods (Missoula floods) inundated and scoured the study area with mud, sand, and gravel (Waitt, 1985). The 233 m thick fine grained sequence of fluvial and lacustrine Neogene sediments in the Tualatin basin comprises the Hillsboro Formation (Wilson, 1997, 1998). The CRBG occupies 300-335 m of the total vertical section of post-Eocene basin fill in the Tualatin basin (USGS CRBG Database; Table A1), underlain by up to ~5.3 km of marine sedimentary rocks and tuffaceous mudstone, siltstone, and minor sandstone of the Yamhill Formation (Yeats et al., 1996; McPhee et al., 2014) (Figure 3.9).

Faulting in the study area is predominantly characterized by northwest trending dextral strike slip faults that include the Sylvan-Oatfield, Portland Hills, East Bank, Canby-Molalla and Gales Creek faults (Yeats et al., 1991, 1996; Blakely et al., 2000). A dextral sense of motion on these faults is compatible with the fault orientations and modern stress field where the maximum horizontal compressive stress is oriented roughly north-south, essentially 45° oblique to the northwest trending faults (Werner, 1990; Yeats et al., 1991). Anderson's theory of faulting shows that these faults are optimally oriented in the current stress regime to experience dextral slip (Anderson, 1905, 1963). Seismicity in the study area since 1969 has been low, with no M > 4 earthquakes recorded in or on the margins of the Portland basin (Blakely et al., 2000). However, the March 25th, 1993 M 5.6 Scotts Mills earthquake that occurred ~58 km south of Portland suggests that the region may still be still seismically active (Thomas et al., 1996; Givler et al., 2009). The Gales Creek fault west of the study area shows evidence for Quaternary activity (Figure 1.1) (Redwine et al., 2017; Wells et al., 2018; Horst et al., 2019), as clockwise rotation and northward migration of the Oregon Coast Range results in dextral shear on faults in the study area and across the forearc (McCaffrey et al., 2007; Wells and McCaffrey, 2013).

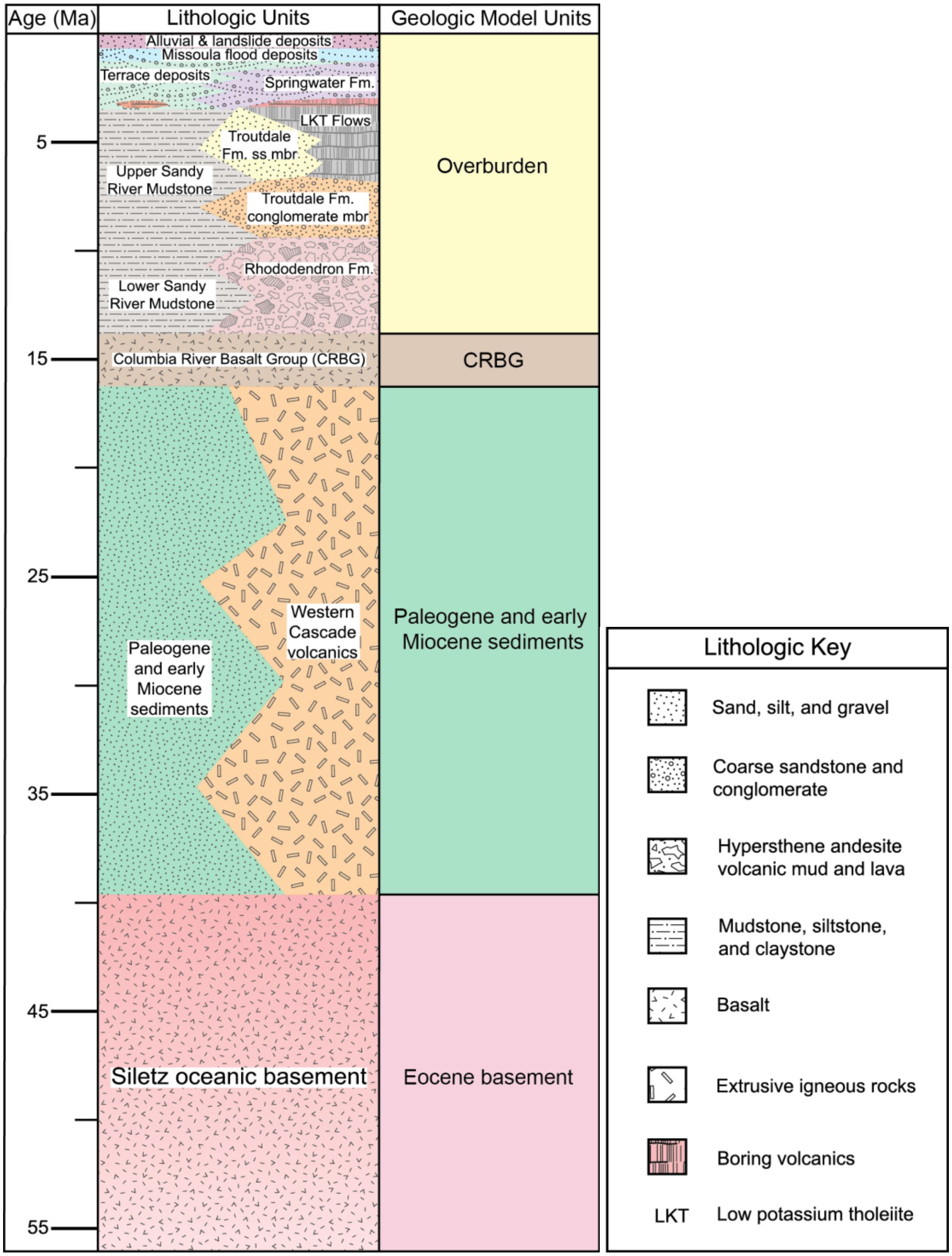

Figure 1.2. Relationship between mapped geology in the Portland and Tualatin basins and geologic model units of this study. Lithologic units schematically depict their spatial distribution in the study area, with west-southwest to the left and east-northeast to the right. Adapted from Evarts et al., (2009b) and Burns et al., (2011).

CHAPTER 2: METHODOLOGY

2.1 Data sources

We model three key stratigraphic horizons in the Portland and Tualatin basins (top CRBG, base CRBG, and Eocene basement) using well log, outcrop, seismic, aeromagnetic, and gravity data. Lithologic data from surface geology and well logs play a crucial role in characterizing subsurface geology. The majority of water wells for the Portland and Tualatin basins are accessed from the Oregon Water Resources Department (OWRD) Groundwater Site Information System (GWIS). Water wells for the Washington State portion of the Portland basin are accessed from the Washington Department of Natural Resources (DNR) and Department of Ecology (DOE). Oil and gas exploration wells used in this study are accessed through the Oregon Department of Geology and Mineral Industries (DOGAMI) oil and gas index. Geologic interpretations of well logs are accessed through the USGS CRBG stratigraphy database. Links to the aforementioned data sources are included in Table A1 of the Appendix.

2.2 Modeling geologic units

Model outputs for this study cover ~3,885 km^2 of the Portland and Tualatin basins (Figure 2.3). The relationship between regional stratigraphy and the geologic units modeled in this study are shown in Figure 1.2. A geologic workflow similar to that in Burns et al. (2011) is employed, in which all available data is compiled as inputs for trend surface (horizon) generation (Figure 2.1). Where data is scarce, subsurface models are largely built on interpretation and interpolation techniques (Tacher et al., 2006).

Modeling horizons is an iterative process, as data density changes both horizontally and vertically throughout the study area (Roe and Madin, 2013).

The rules of interpolation between known points are highly variable and prescribed by the method selected (Burns et al., 2011). Kingdom Suite, a geological interpretation software from IHS Markit, is utilized in this study to generate a series of structure and isochore maps. Kingdom's Flex Gridding uses a system of differential equations whose solution yields a grid of points that must pass through (or very close) to the data in XYZ space.

Residual values are defined as the difference between the formation top elevation and the elevation predicted by the interpolation method prescribed. Values are positive if the data is higher than the interpolated surface and negative if lower (Burns et al., 2011). To test the utility of the Flex Gridding method, a map of residuals for a test horizon (top CRBG) is generated using both the Flex Gridding and Natural Neighbor interpolation methods. The Natural Neighbor method results in widely variable residuals across the study area, whereas the Flex Gridding method does a better job of fitting the interpolated formation top values (Figures A2, A3). Given that data can be sparse in certain portions of the study area (i.e., southeast Portland basin), it is important that the resulting grid passes through (or at least very close) to what few control points exist in such regions.

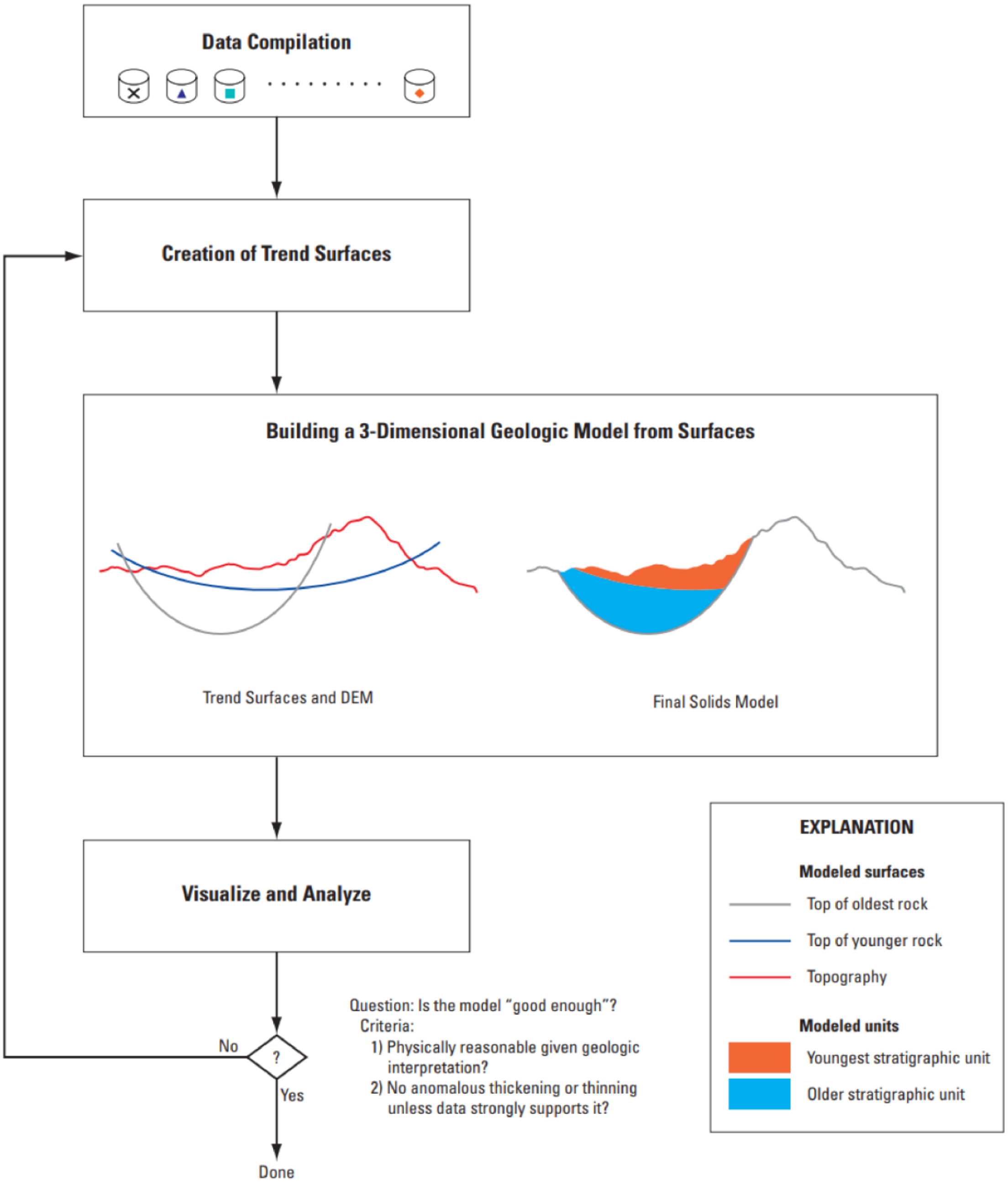

Figure 2.1. General geologic modeling workflow, after Burns et al. (2011).

2.2.1 Top CRBG

A total of 2,336 wells are used to model the top of CRBG in this study (Supplemental Data Table 1). Stratigraphic picks for the top of CRBG are reviewed and verified. Confirming lithologies and correlations between well logs ensures data integrity. Well names, surface elevations, and stratigraphic picks can be found in the Excel spreadsheet included as a supplemental file (Supplemental Data Table 1). Water wells in the Portland and Tualatin basins have been used to characterize post-CRBG (< 15 Ma) sedimentary overburden (McCarthy and Anderson, 1990; Swanson et al., 1993; Wilson, 1997; Orzol et al., 2000; Roe and Madin, 2013). While useful in understanding the stratigraphy of shallow aquifers, many of the wells contained in these datasets do not penetrate the top of CRBG. However, the deepest of these wells provide minimum elevation estimates of CRBG. The best well log control for the top of CRBG exists along the margin of the basins, where depths required to reach this unit are relatively shallow. In addition to well data, seismic profiles in both basins are used to estimate top CRBG elevations (Popowski, 1996; Liberty, 2002). Outcrop data surrounding the basins are integrated using a new regional geologic map of the study area superimposed onto a 10 meter resolution digital elevation model (DEM) (Wells et al., 2018). The topographic elevation of geologic units exposed at the surface represents the top (or bottom) of the unit (Burns et al., 2011). Short-wavelength aeromagnetic anomalies caused by surface and near-surface presence of CRBG and geologic field relations help delineate the eastern boundary of CRBG in the Portland basin (Blakely et al., 1995, 2000; Ray Wells, personal comm.).

2.2.2 Base CRBG

Data availability tends to decrease with depth, so that deeper stratigraphic surfaces are not as well constrained. Roe and Madin (2013) note that few drill holes penetrate this unit and even fewer reach the base of CRBG as a function of the thick weathered surface of the CRBG, the tendency of drillers to stop when hard rock is reached, and limited urban development where CRBG is exposed. A total of 52 wells were used to model base CRBG in this study (Supplemental Data Table 1). While only 4 of the 11 wells penetrate the entire CRBG section, the remaining 7 wells reach into the Wapshilla Ridge unit and are interpreted to be close to base of CRBG based on stratigraphy (Beeson et al., 1989a). A detailed stratigraphic column of the CRBG can be found in Figure A1 of the Appendix. Given that pre-existing topography largely controlled the distribution of CRBG flows, thicker flow units represent topographic lows in the mid-Miocene and thinner units topographic highs (Beeson et al., 1989a). Seismic and well log data in the Tualatin basin are used to estimate the thickness of CRBG along a 2D seismic line shot along the Columbia River in the Portland basin (see section 2.4. Generating isochore maps). The base of CRBG is exposed along the margins of the Tualatin basin and around the Dutch Canyon anticline (Figure 1.1). As with the top CRBG horizon, these surficial geologic contacts are used to guide interpolation. Gravity data is also used to interpret base CRBG elevations, where thinner flows overlie gravity (basement) highs and thicker flows overlie gravity lows (McPhee et al., 2014). Exposures of pre-CRBG sedimentary rock and basement (i.e., Waverly Heights, southwest flank of the Portland Hills, and Dutch Canyon) provide additional constraints on the thickness and areal extent of this unit in the study area.

2.2.3 Eocene basement

As there are few wells that penetrate Eocene basement, modeling of the basement surface relies heavily on the gravity inversion grid of McPhee et al. (2014). The extent of the inversion in relation to the study area is shown in Figure 3.5. The gravity-derived depth to basement map is inconsistent with top and base CRBG surfaces in the southeastern portion of the Portland basin, where basement crosses the overlying top and base CRBG horizons. The gravity derived basement surface is too shallow in this region due less dense western Cascades arc rock at depth. As a result, gravity measurements in this area can be erroneous. McPhee et al. (2014) note that the determination of basement depth is poorly constrained in this region and suggests that Paleogene Cascade Volcanic arc rocks, which are less dense than the basement assumed in the inversion, may underlie much of the Portland basin. Areas of uncertainty in the basement grid are indicated on structure and isochore maps. Areas where Eocene basement is exposed (i.e., Waverly Heights basalt) provide critical constraints for both the gravity inversion and understanding the geometry of overlying units in the vicinity (Beeson et al., 1989b).

2.3 Modeling faults

Major faults in the study area are modeled as sub-vertical planes. These include the Beaverton, Canby-Molalla, and Sylvan-Oatfield faults in the Tualatin basin and Portland Hills, East Bank, Prune Hill/Blue Lake and Lacamas lake faults in the Portland basin (Figure 2.4). The majority of displacements on the Sylvan-Oatfield, Portland Hills, and East Bank faults are likely taken up in dextral strike-slip motion (Blakely et al., 1995, 2000, 2004). Each fault surface is modeled down to Eocene basement, where offsets in the gravity inversion grid can be correlated to mapped faults at the surface.

2.4 Generating isochore maps

Isochore maps show the spatial variability of unit thickness over the study area (see section 3.2. Isochore maps). Three isochore maps are generated for three representative time intervals (i.e., horizons): (1) post-CRBG sedimentary overburden (0-15 Ma), (2) mid-Miocene Columbia River Basalt Group (CRBG, 15.5-16.5 Ma), and mid-Miocene to late Eocene (~ 17-35 Ma) time. Each isochore map is computed as the difference between a geologic unit's top surface and its bottom using a map subtraction function in IHS Kingdom Suite. As in Burns et al. (2011), interpolation guides are introduced into the modeling process to create surfaces that are consistent with geologic conceptual models and what can be inferred from geological and geophysical data (Roe and Madin, 2013) (Figure 2.2).

The CRBG isochore map is based partly on multichannel seismic reflection data in the Tualatin basin. The seismic data was collected in 1984-85 as part of a search for petroleum in the area (Popowski, 1996). Based on well and outcrop data, thickness values for CRBG are similar in both basins. Seismic data is correlated to nearby wells (WASH 55816, Cooper Mt.) that penetrate ~305 to 323 m of CRBG (Supplemental Data Table 1). CRBG thickness ranges from 0.1 to 0.15 two-way travel time (TWT) on the seismic lines (Popowski, 1996). Using the well data, a seismic velocity of ~5,300 m/s is estimated, and a TWT ratio of 0.125 seconds = ~335 m is used. This velocity value is consistent with Spitzer et al. (2008), who document a seismic velocity of ~4.5 km/s (4,500 m/s) to ~5.8

km/s (5,800 m/s) for flood basalts on the Faroes margin and Faroe-Shetland basin in the North Atlantic Ocean. Using the Tualatin basin as an analog, we estimate the thickness of CRBG in the Portland basin. Minimum thicknesses are constrained where CRBG is exposed (Wells et al., 2018).

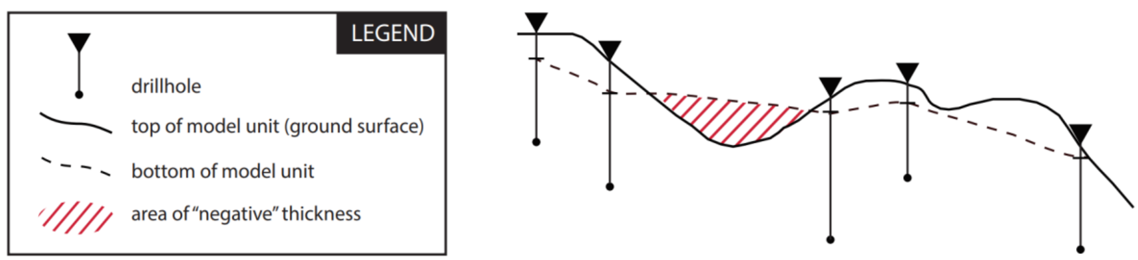

Figure 2.2. Schematic illustrating a situation in which the bottom horizon of a model unit is interpolated above a higher resolution top. Introducing interpolation guide points rectifies this erroneous thickness results in more reasonable structure and isochore maps. After Roe and Madin, 2013.

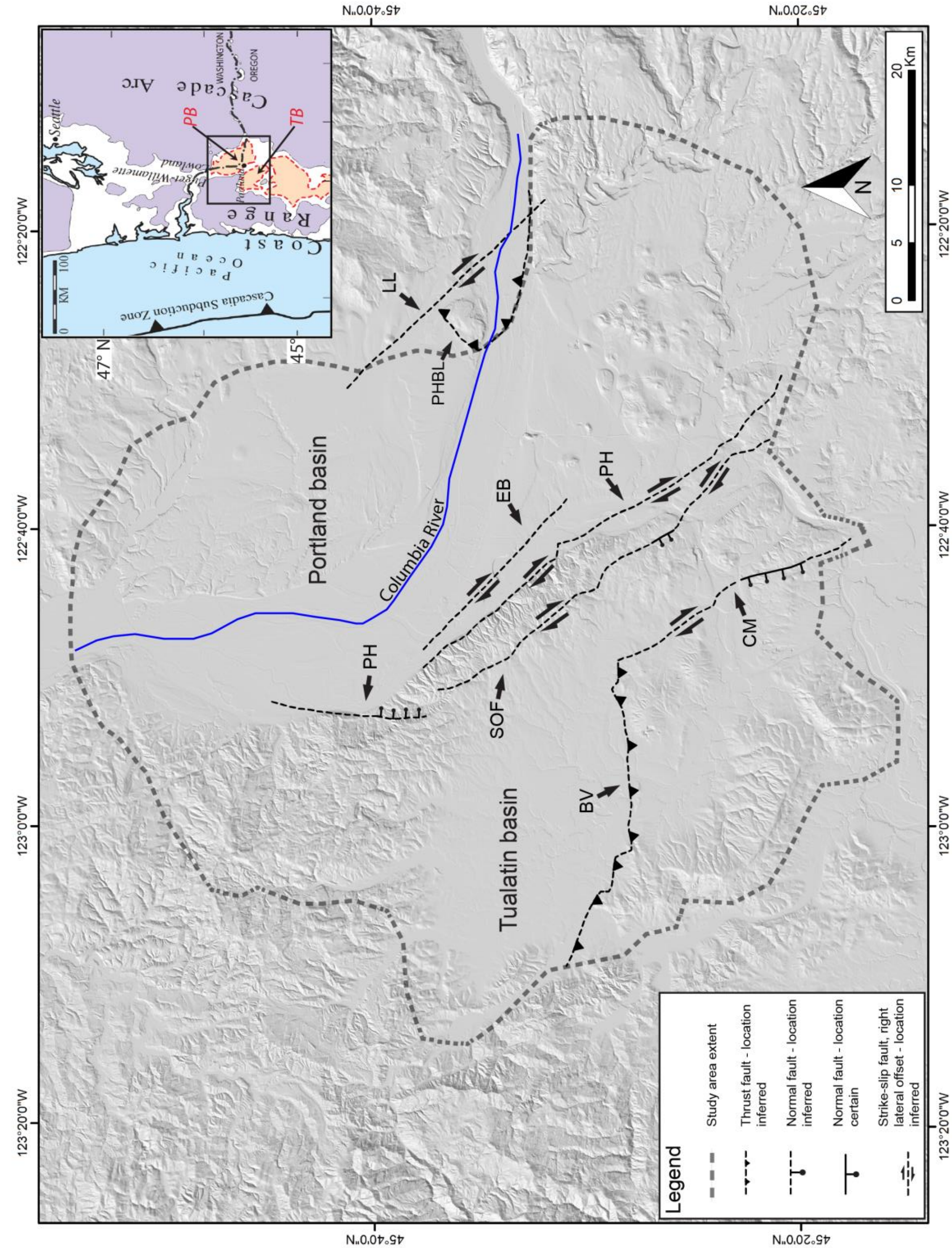

Figure 2.3. Major faults included in the basin model, from Wells et al., 2018. BV – Beaverton fault; CM – Canby-Molalla fault; SOF – Sylvan-Oatfield fault; PH – Portland Hills fault; EB – East Bank fault; PHBL – Prune Hill/Blue Lake fault; LL – Lacamas Lake fault. Inset: PB – Portland basin; TB – Tualatin basin.

CHAPTER 3: RESULTS

3.1 Structure maps

Structure maps (surface horizons) generated for top CRBG, base CRBG, and Eocene basement reveal basin geometry including faults and folds in the study area (Figures 3.2, 3.4, 3.6). Maps that show the spatial distribution of data used to model each surface are included for reference (Figures 3.1, 3.3, 3.5). A description of the major structural features of each surface follows.

3.1.1 Top CRBG

The top CRBG horizon is relatively well constrained due to the large amount of subsurface data available (Figure 3.1). This surface reveals two distinct synclines delineating the Portland and Tualatin basins separated by a large northwest trending anticline associated with the Portland Hills (Figure 3.2). The surface reaches a greater depth in the Portland basin of -1640 ft (-500 m) elevation compared to the Tualatin basin which is -1279 ft (-390 m).

The top CRBG horizon is exposed at the surface throughout the study area (Wells et al., 2018) (Figure 1.1). The elevation of the top CRBG surface reaches a maximum elevation of ~2100 ft (640 m) outside of the modern basin at Dutch Canyon, northwest of the Portland Hills. Structure map rugosity reflects the resolution of the regional DEM in areas where CRBG is exposed at the surface, particularly along the Portland Hills, Dutch Canyon, and the margins of the Tualatin basin. Modeled faults are coincident with steep gradients on the structure map (Figure 3.2). The Portland Hills anticline is bound by the

Sylvan-Oatfield and Portland Hills dextral strike slip reverse faults, with an anticline separating the two basins (Figure 3.2). An inferred extension of the Portland Hills fault offsets the Portland basin syncline down to the southeast. Elevation decreases markedly northeast of the East Bank fault, with a gently sloping surface between it and the Portland Hills fault (Figure 3.2). The edge of the top CRBG surface terminates against the dextral Lacamas Lake and reverse Prune Hill/Blue Lake faults on the eastern side of the Portland basin (Figure 2.3). A CRBG anticline in the Tualatin basin, Cooper Mountain, is in the hanging wall of the Beaverton thrust (or reverse) fault reaching a maximum elevation of ~698 ft (213 m). This is nearly ~1968 ft (600 m) higher than the same surface in its footwall to the north (Figure 3.2). South of the Beaverton fault, the Tualatin basin consists of multiple blocks of faulted CRBG and, while data exists for this horizon, it is structurally complex and beyond the scope of this study. This area is denoted by a diagonal-hatch pattern on the top and base CRBG maps (Figures 3.2, 3.4). The dextral Canby-Molalla fault (Blakely et al., 2000) links up with the Beaverton fault to the southeast, defining the eastern edge of this domain.

There are a few locations in the study area where CRBG is missing, and pre-CRBG sedimentary rock is exposed at the surface. These areas are denoted with a cross-hatch pattern (Figure 3.2). Dutch Canyon, the core of an eroded anticline, exposes older Paleogene and early Miocene sediments at the surface. These same sediments are exposed in a small area on the southwest flank of the Portland Hills along the Sylvan-Oatfield fault. CRBG is also missing where Eocene basalt is exposed south of the Portland Hills near Waverly Heights (Figure 1.1).

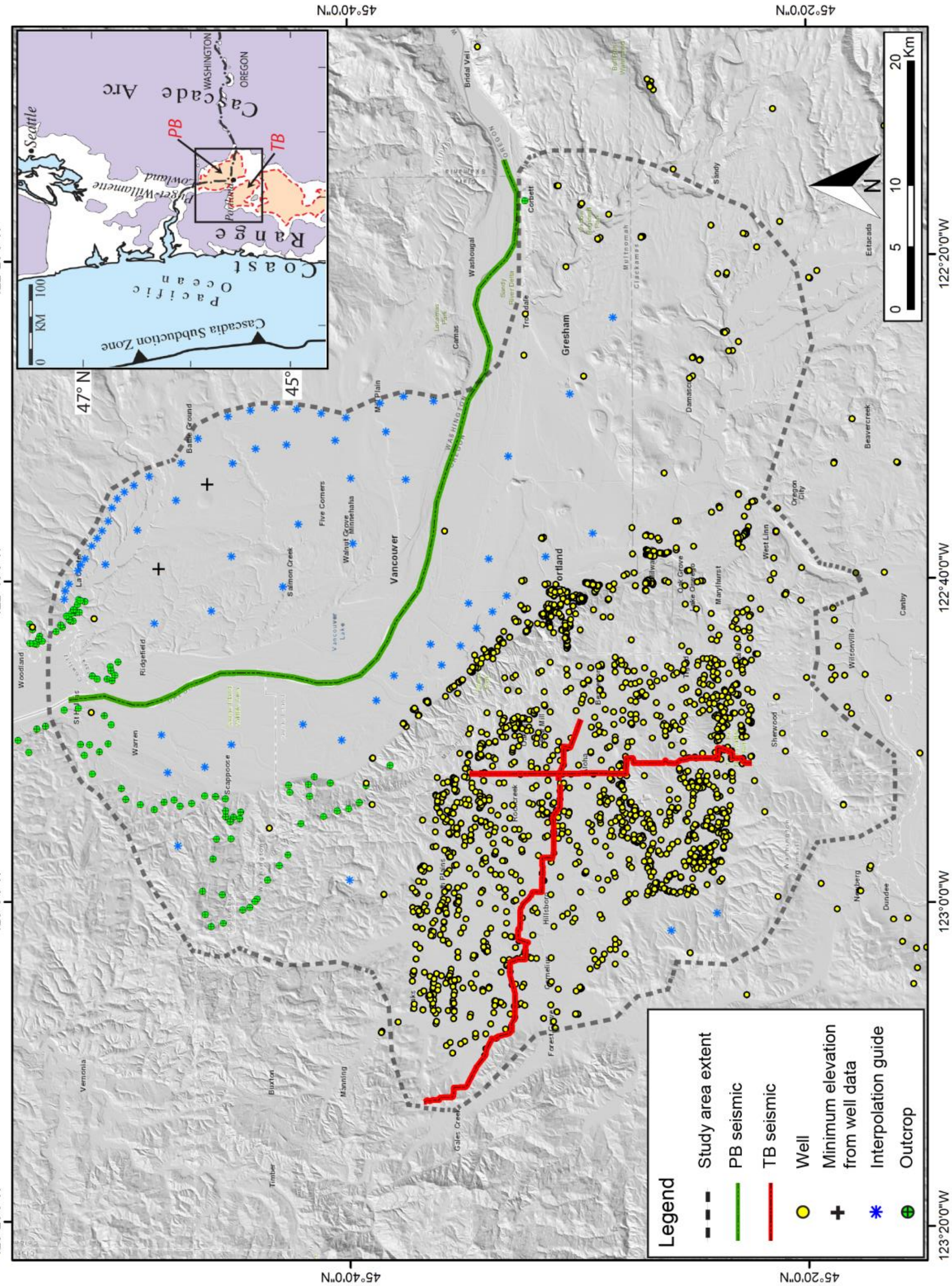

Figure 3.1. Data control on the top CRBG structure (surface) map (Figure 3.2). Interpolation guides (star symbol) prevent surface cross-over in areas with sparse data availability (Figure 2.2). Inset: PB – Portland basin; TB – Tualatin basin.

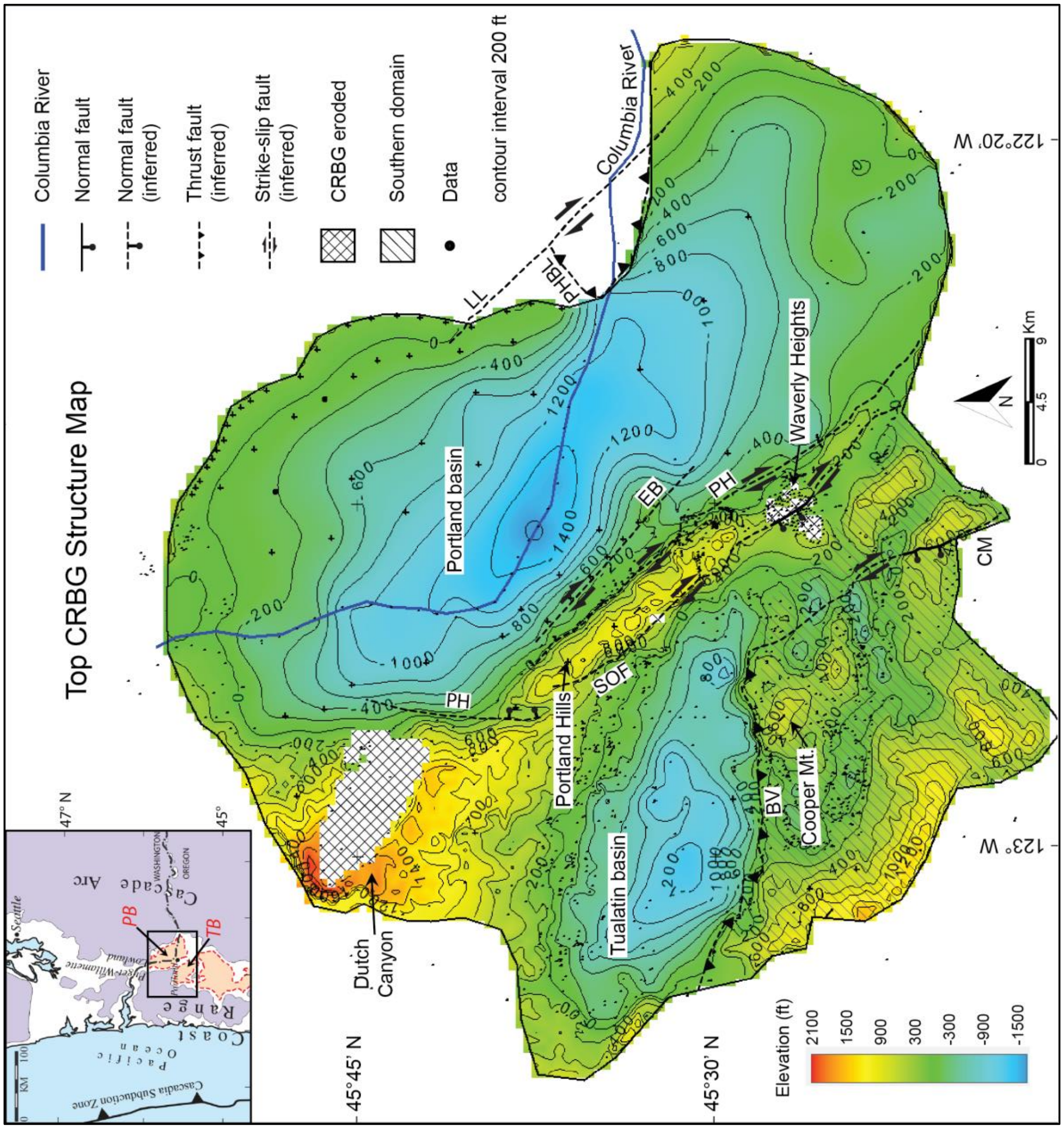

Figure 3.2. Structural contour map of top CRBG. The top CRBG surface is exposed along the Portland Hills anticline, which separates the Portland and Tualatin basins, and along the southwestern margin of the Tualatin basin. These areas are highlighted by higher elevations (yellow shading), adjacent to lower elevation basins (blue shading). Contour interval = 200 ft. Location of the Columbia River shown for reference. BV – Beaverton fault; CM – Canby-Molalla fault; SOF – Sylvan-Oatfield fault; PH – Portland Hills fault; EB – East Bank fault; PHBL – Prune Hill/Blue Lake fault; LL – Lacamas Lake fault. Inset: PB – Portland basin; TB – Tualatin basin.

3.1.2 Base CRBG

Compared to the top of CRBG, the base CRBG horizon is poorly constrained due to the sparse amount of data that penetrates the horizon in the subsurface (Figure 3.3). The structure of base CRBG reflects that of the top CRBG, with two synclines delineating the Portland and Tualatin basins separated by the Portland Hills anticline (Figure 3.4). This surface also reaches greater depths in the Portland basin at -2690 ft (-820 m) relative to the Tualatin basin which is -2395 ft (-730 m). The surface reaches a maximum elevation of ~1870 ft (570 m) at Dutch Canyon.

Modeled faults are generally coincident with steep elevation gradients on the structure map (Figures 2.3, 3.4). The Sylvan-Oatfield and Portland Hills faults bound a northwest trending structure of higher elevation coincident with the Portland Hills. The inferred northwest extension of the Portland Hills fault matches a steep gradient that offsets the Portland basin syncline down to the southeast. Similar to the top CRBG surface, elevation decreases markedly northeast of the East Bank fault, with a gently sloping surface between it and the Portland Hills fault (Figure 3.4). At the location of Cooper Mountain in the Tualatin basin, this surface reaches a maximum elevation of ~ -328 ft (-100 m) in the hanging wall of the Beaverton thrust fault, and decreases to -1601 ft (-488 m) in its footwall to the north (Figure 3.4).

The base CRBG horizon is exposed at the surface in a few locations in the study area, chiefly around the west-southwest margin of the Tualatin basin, Dutch Canyon, and the southwest flank of the Portland Hills (Wells et al., 2018). Exposed pre-CRBG sedimentary rock is denoted with a cross-hatch pattern (Figure 3.4).

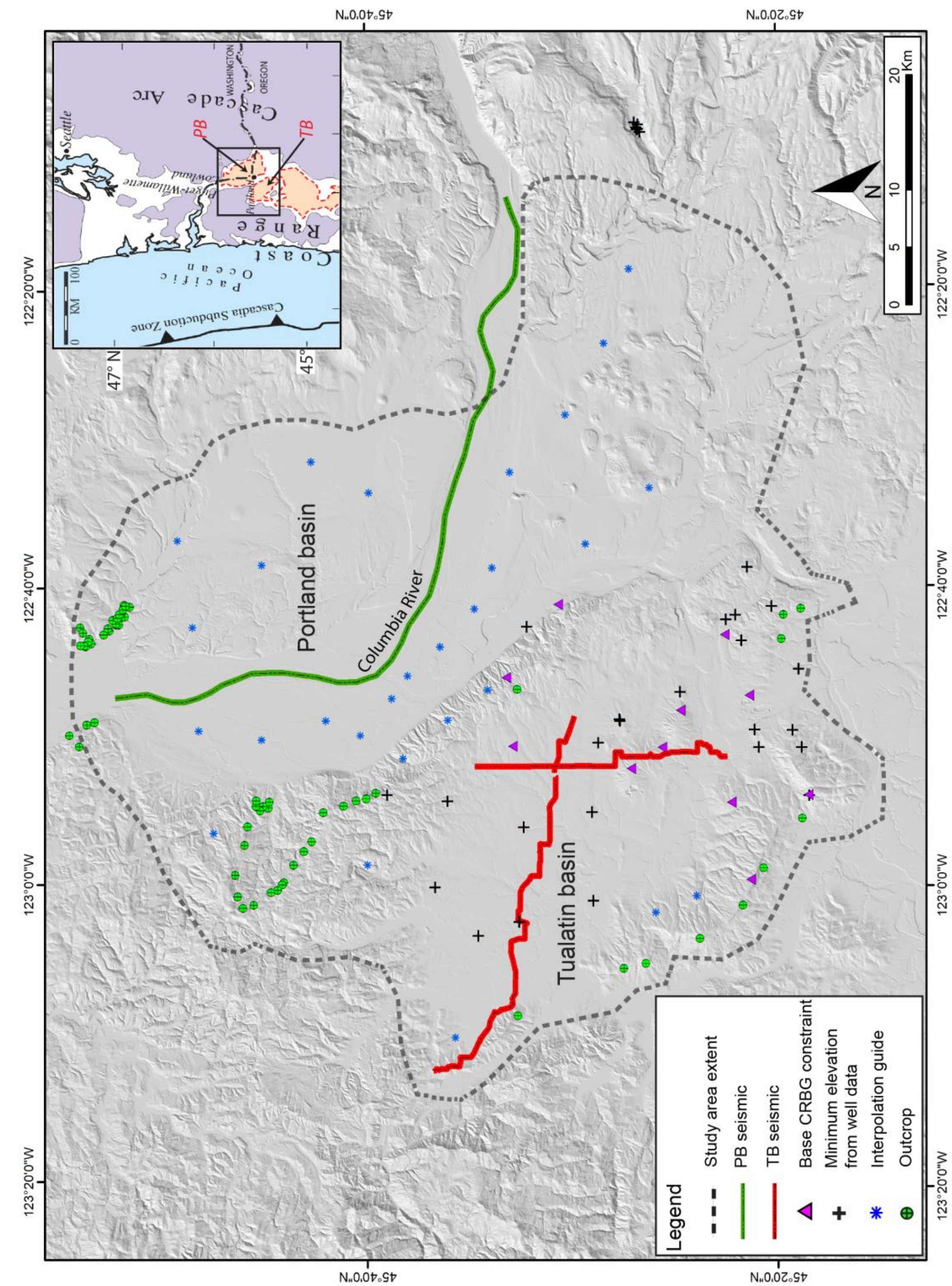

Figure 3.3. Data control on the base CRBG structure (surface) map (Figure 3.4). Base CRBG constraints (triangle symbol) are from the USGS CRBG stratigraphy database, which includes the majority of the deepest wells in the study area (Table A1). Interpolation guides (star symbol) prevent surface cross-over in areas with sparse data availability as shown in Figure 2.2. Inset: PB – Portland basin; TB – Tualatin basin.

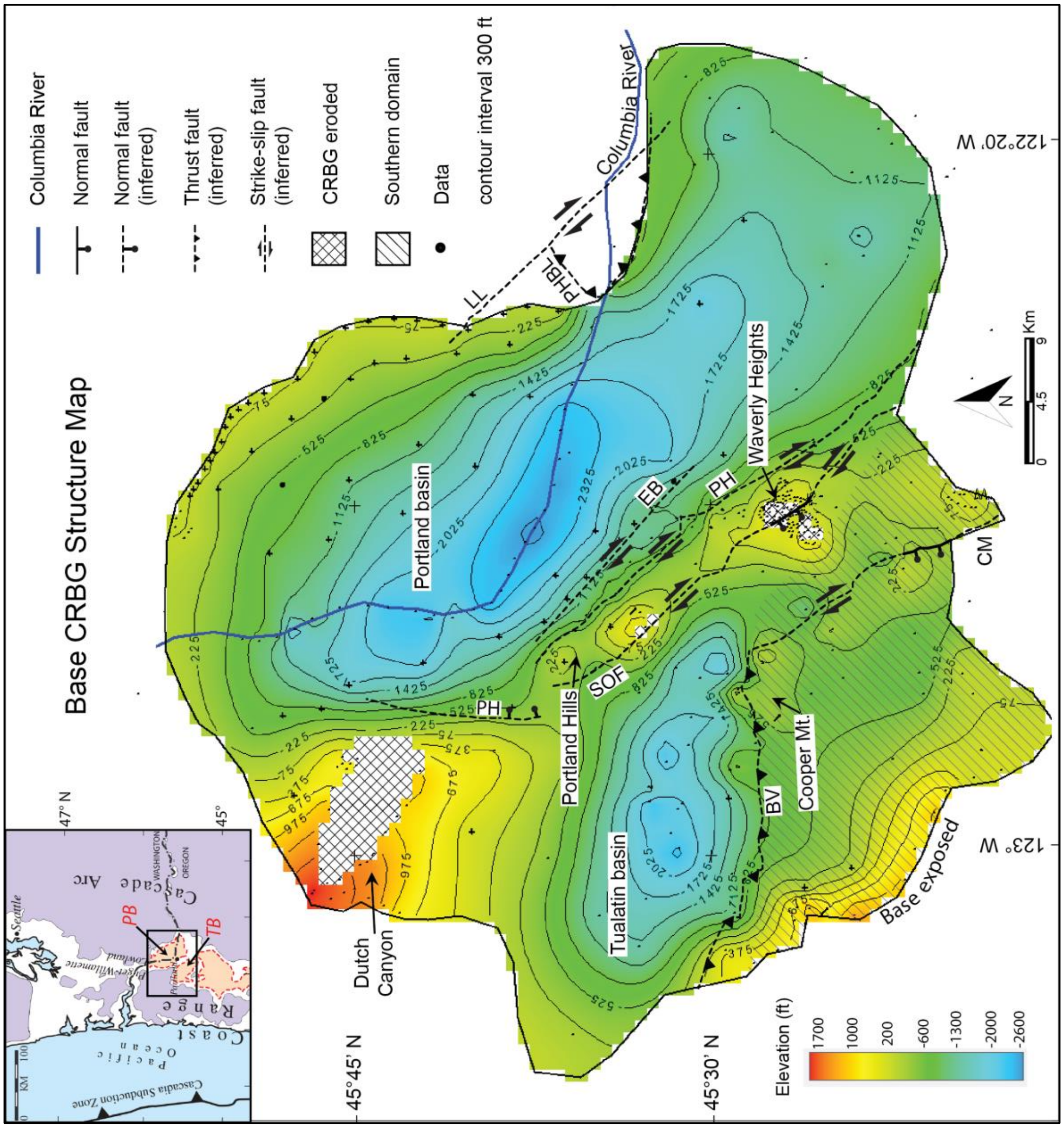

Figure 3.4. Structural contour map of base CRBG. Regions of higher elevation (yellow shading) along the Portland Hills separates the Portland and Tualatin basins. The base CRBG surface is exposed around Dutch Canyon and the southwest margin of the Tualatin basin. Contour interval = 300 ft. Location of the Columbia River shown for reference. BV – Beaverton fault; CM – Canby-Molalla fault; SOF – Sylvan-Oatfield fault; PH – Portland Hills fault; EB – East Bank fault; PHBL – Prune Hill/Blue Lake fault; LL – Lacamas Lake fault. Inset: PB – Portland basin; TB – Tualatin basin.

3.1.3 Eocene basement

The gravity derived depth to basement grid of McPhee et al. (2014) was imported into Kingdom as a dense grid of XYZ points. The grid covers the entire Tualatin basin, but only a portion of the Portland basin (McPhee et al., 2014) (Figure 3.6). This surface reveals a deep depression underneath the Tualatin basin, which gradually increases in elevation toward the western Cascades to the east (Figure 3.6). The surface is over twice as deep in the Tualatin basin at -18,700 ft (-5.7 km) compared to the Portland basin which is -6,890 ft (2.1 km). Elevation is shallowest in the southern portion of the study area. In the southeastern portion of the Portland basin, western Cascade arc rock is less dense from that assumed for basement in the gravity inversion (McPhee et al., 2014). This causes a shallowing of basement in that area, and is denoted by a diagonal-hatch pattern (Figure 3.6). The surface increases to a local high of ~ -2952 ft (-0.9 km), coincident with the Dutch Canyon anticline.

Modeled faults are also coincident with steep gradients on the Eocene basement structure map, suggesting they deform basement (Figure 3.6). The Sylvan-Oatfield and Portland Hills faults follow two northwest trending basement highs at the boundary between the Portland and Tualatin basins. Basement elevation ranges from ~ -5,577 ft (-1700 m) to ~ -6,889 ft (-2.1 km) in a basement low coincident with the Portland Hills anticline (Figure 3.6). In the Tualatin basin, the basement surface lies at -7,545 ft (-2.3 km) elevation in the hanging wall of the Beaverton fault, decreasing from ~ -11,154 ft (-3.4 km) to ~ -14,763 ft (-4.5 km) in its footwall to the north (Figure 3.6).

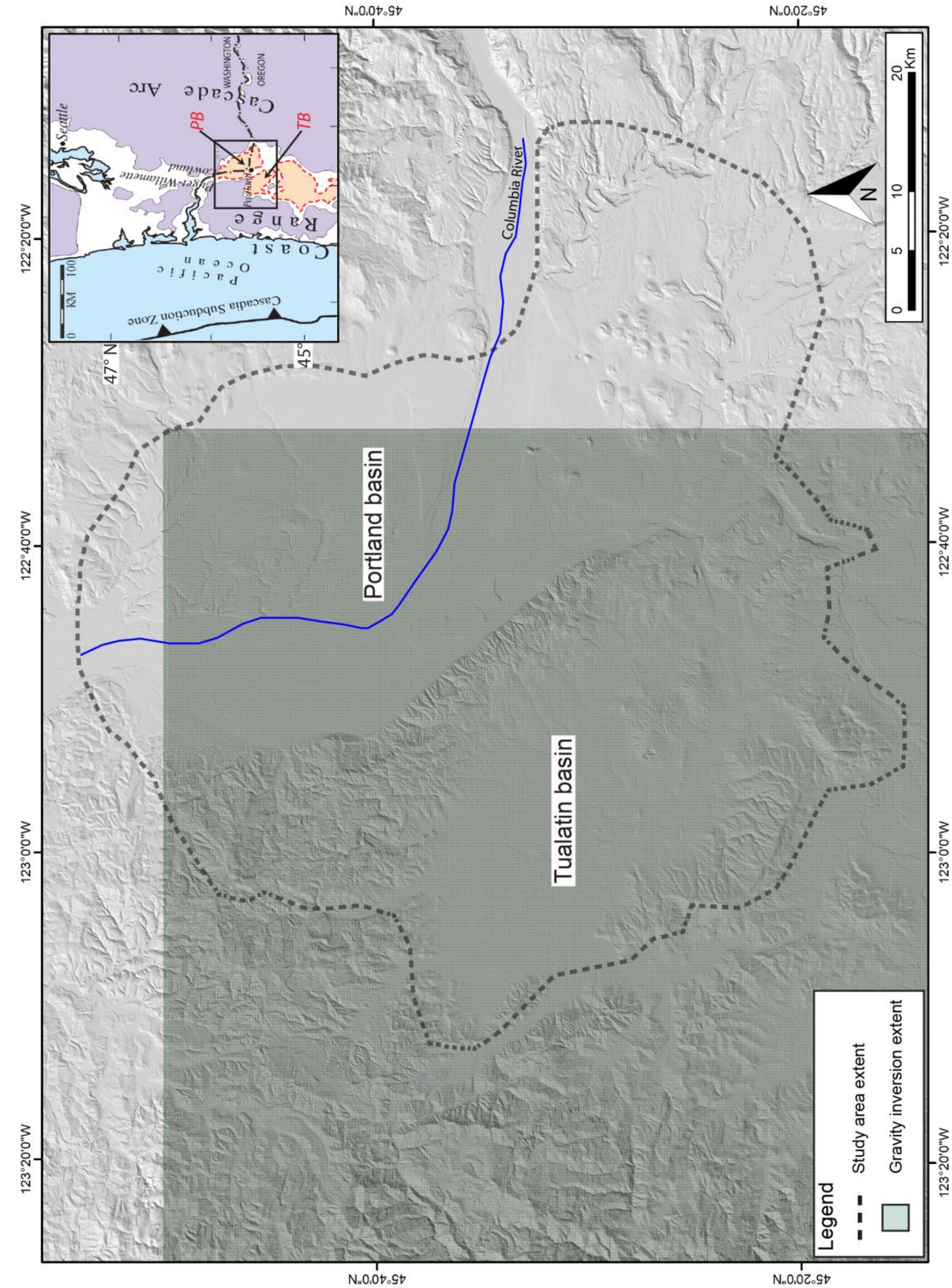

Figure 3.5. Extent of gravity inversion used to constrain Eocene basement in the study area. Note that the grid does not cover the entire Portland basin. Inset: PB – Portland basin; TB – Tualatin basin.

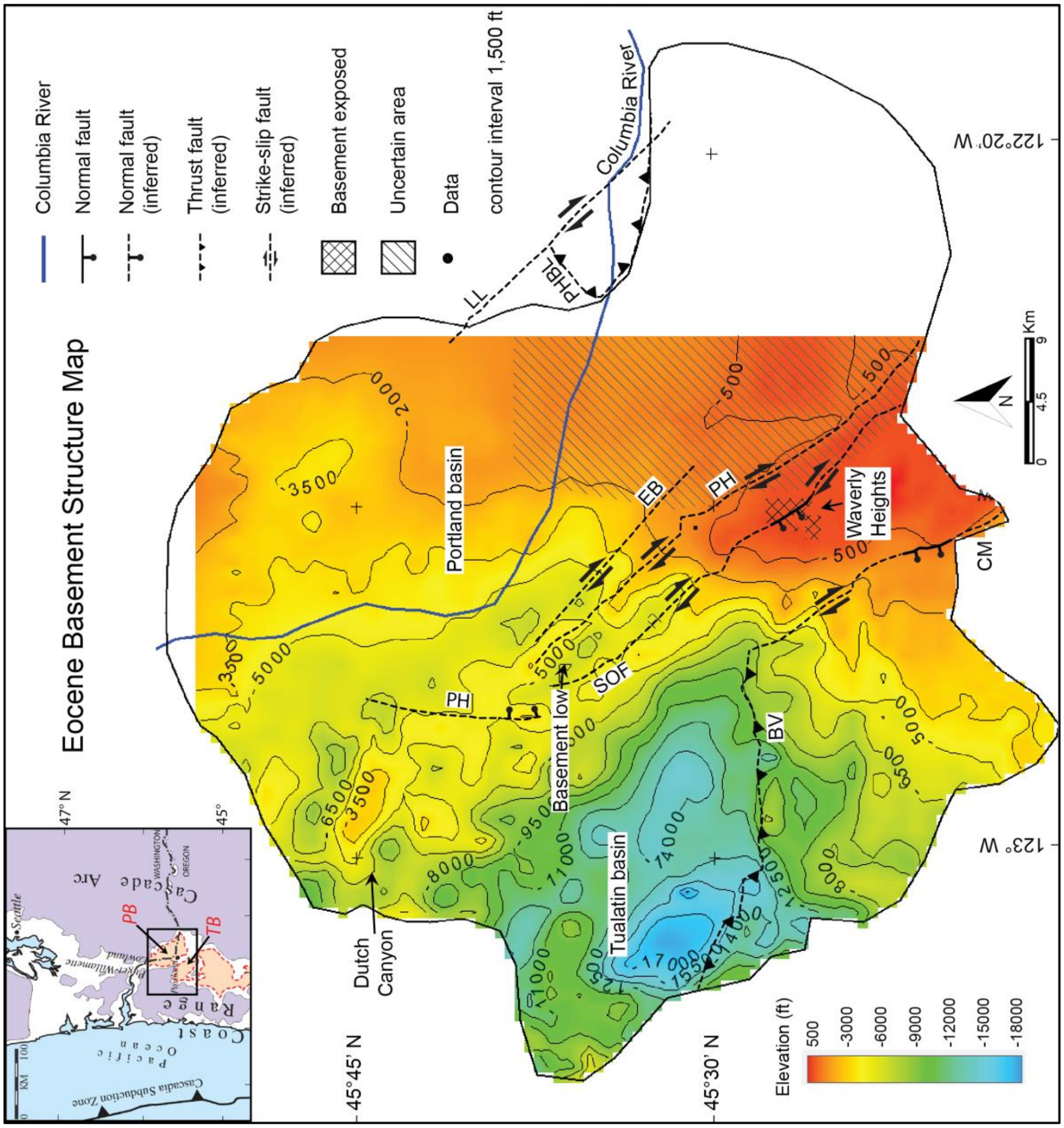

Figure 3.6. Structural contour map of Eocene basement. The elevation is the lowest in the Tualatin basin (blue shading) and shallows to the east across the Portland basin (orange shading). Eocene basement is exposed in the vicinity of Waverly Heights. Contour interval = 1,500 ft. Location of the Columbia River shown for reference. BV – Beaverton fault; CM – Canby-Molalla fault; SOF – Sylvan-Oatfield fault; PH – Portland Hills fault; EB – East Bank fault; PHBL – Prune Hill/Blue Lake fault; LL – Lacamas Lake fault. Inset: PB – Portland basin; TB – Tualatin basin.

3.2 Isochore maps

Isochore maps generated for three representative time intervals (0-15 Ma, 15.5-16.5 Ma, and ~17-35 Ma) reveal depocenter migration as well as local thinning and thickening across the study area. A description of major thickness variations across these intervals follows.

3.2.1 Post-CRBG sedimentary overburden (0-15 Ma)

The post-CRBG sedimentary overburden (0-15 Ma) isochore map reveals two distinct northwest trending depocenters coincident with the Portland and Tualatin basins since mid-Miocene time (Figure 3.7). Thicker sediments were deposited in the Portland basin at ~1,640 ft (500 m) compared to the Tualatin basin which reaches ~1,459 ft (445 m) thick at this time. Sedimentary rocks thin onto the Portland Hills (Figure 3.7) where CRBG is exposed. Isolated “bullseyes” of ~1,410-1,509 ft (430-460 m) thick basin fill in the southern portion of the Portland basin are volcanic cones of the post-CRBG Boring Volcanic field. Relatively thick sedimentary deposits in the southernmost portion of the Portland basin reflect its continuation into the Northern Willamette basin (Figures 1.1, 3.7).

Modeled faults in the study area mark abrupt changes in 0-15 Ma sediment thickness (Figure 3.7). The inferred northeast extension of the Portland Hills fault reveals a steep thickness gradient on its footwall and negligible thickness on its hanging wall. In Figure 3.7, this is shown along the fault trace southeast of Dutch Canyon. The East Bank fault bounds a steep thickness gradient to its northeast, shown by the transition in Figure 3.7 from warm colors (thick sediment package) to the northeast to cool colors (thin sediment package) to the southwest. A significant change in thickness is also observed across the Beaverton fault in the Tualatin basin (Figure 3.7).

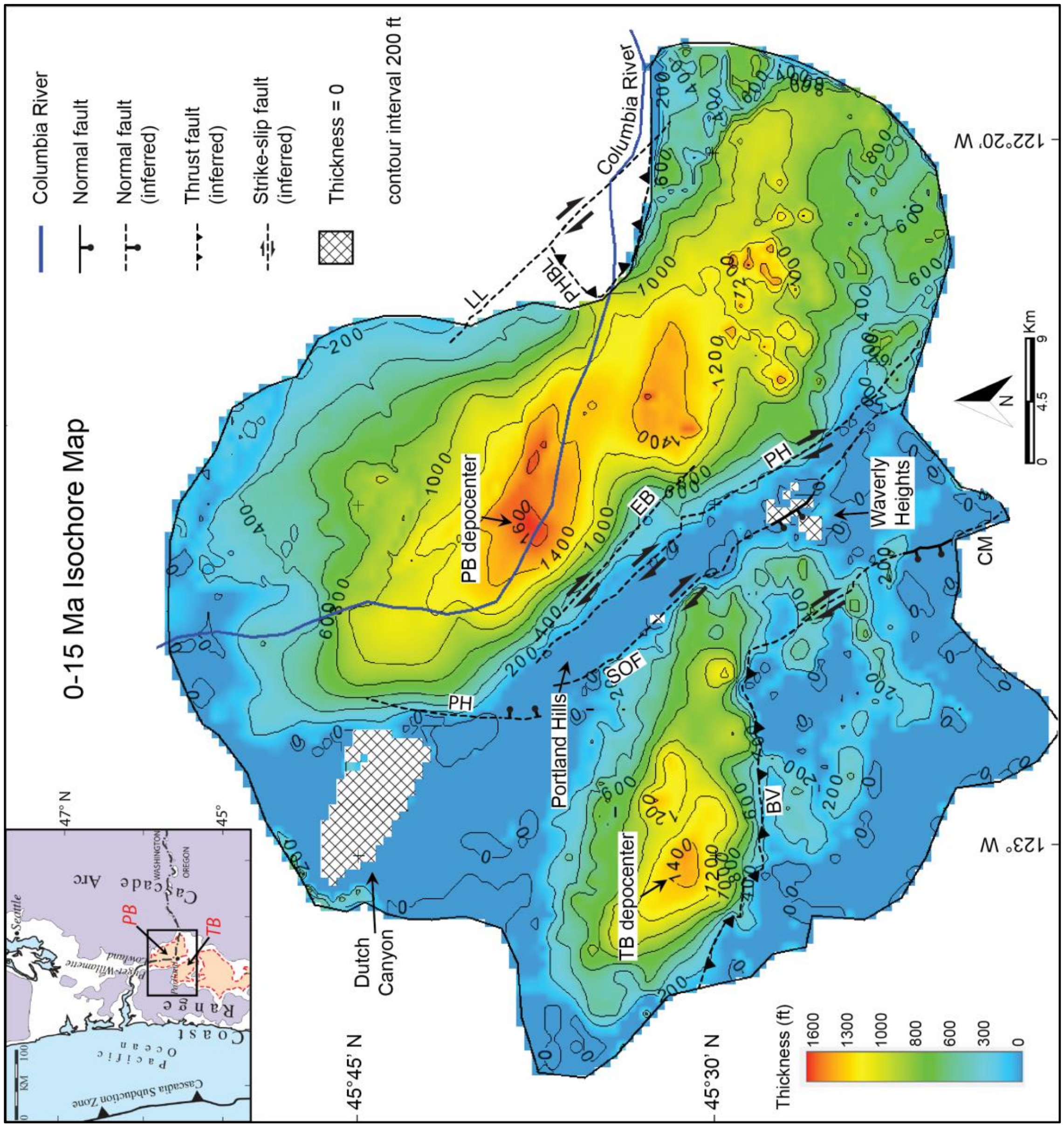

Figure 3.7. Post-CRBG sedimentary overburden (0-15 Ma) isochore map generated as the difference between DEM derived topography and top CRBG structure map. The northeast extension of the Portland Hills fault is shown southeast of Dutch Canyon. Thickness packages less than ~ 1 km diameter are likely an interpolation artifact. Contour interval = 200 ft. Location of the Columbia River shown for reference. BV – Beaverton fault; CM – Canby-Molalla fault; SOF – Sylvan-Oatfield fault; PH – Portland Hills fault; EB – East Bank fault; PHBL – Prune Hill/Blue Lake fault; LL – Lacamas Lake fault. Inset: PB – Portland basin; TB- Tualatin basin.

3.2.2 Mid-Miocene Columbia River Basalt Group (15.5-16.5 Ma)

The CRBG (15.5-16.5 Ma) isochore map reveals multiple depocenters across the mid-Miocene Portland and Tualatin basins, with the basalt thinning and thickening in multiple locations around the study area (Figure 3.8). On average, thickness of CRBG is comparable between the two basins, with ~902-1,085 ft (275-330 m) in the Portland basin and ~902-1,197 ft (275-365 m) in the Tualatin basin (Figure 3.8). CRBG remains relatively thick south of the Portland basin. The basalt thins to its inferred easternmost extent at the foothills of the western Cascades. It also thins around Waverly Heights and Dutch Canyon (Figure 3.8).

An area of local thickening coincident with the Portland Hills is bound by the Sylvan-Oatfield and Portland Hills faults (Figure 3.8). Here, the basalt ranges from ~705-984 ft (215-300 m) thick. Along the trace of the faults, the basalt thins to ~295-590 ft (90-180 m) before thickening towards the central Portland and Tualatin basins (to the east and west, respectively). The East Bank fault juxtaposes an area of thick basalt to the northeast, against basalt that is 200-400 ft (~60-120 m) thinner to the southwest (Figure 3.8). Relatively thick CRBG exists north of the Beaverton fault and to the south near Cooper Mountain (Figure 3.8), though model uncertainty in this area is high (see section 3.1. Structure maps).

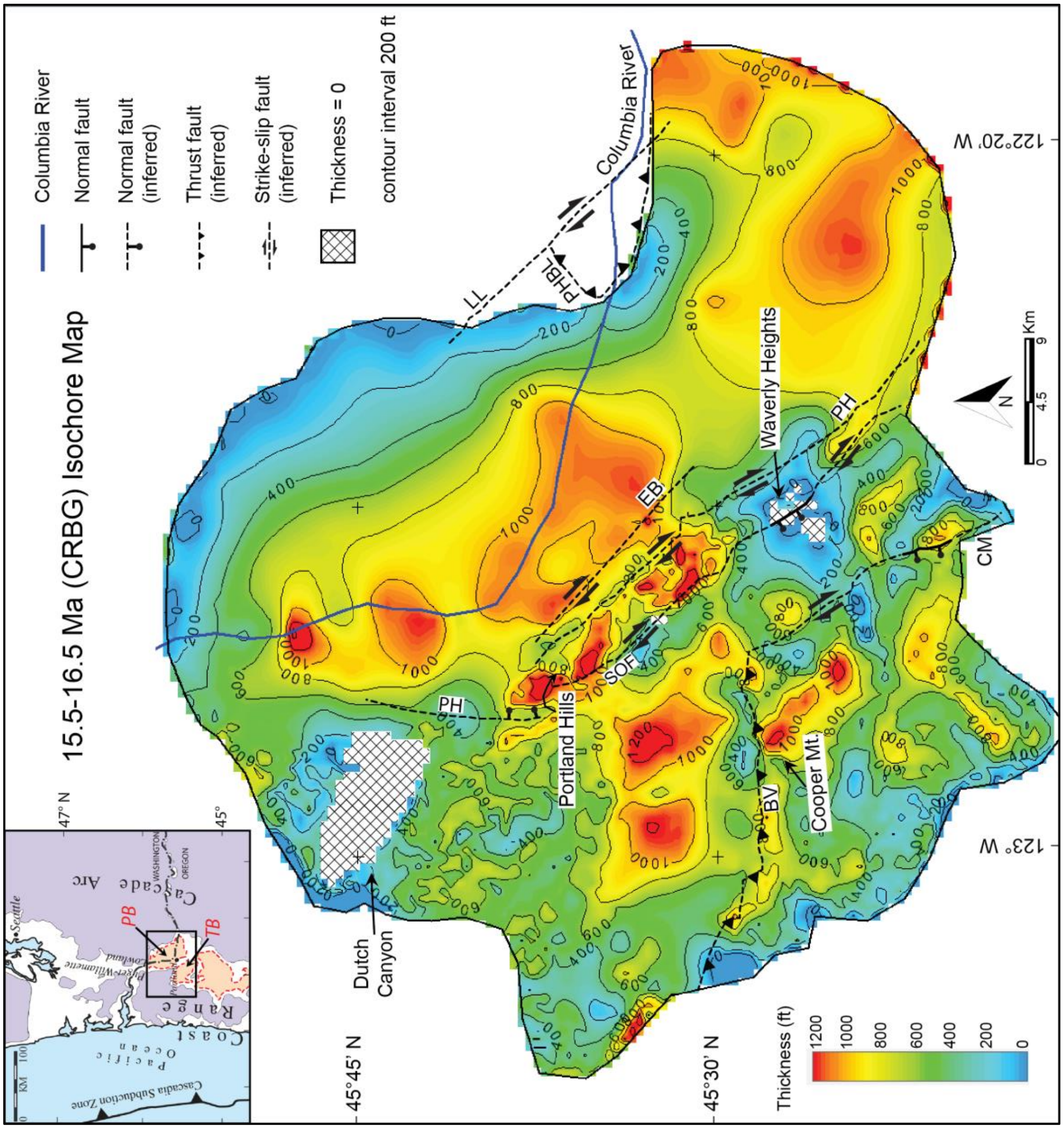

Figure 3.8. Mid-miocene CRBG (15.5-16.5 Ma) isochore map generated as the difference between the top and base CRBG structure maps. Thickness packages less than ~ 1 km diameter are likely an interpolation artifact. Contour interval = 200 ft. Location of the Columbia River shown for reference. BV – Beaverton fault; CM – Canby-Molalla fault; SOF – Sylvan-Oatfield fault; PH – Portland Hills fault; EB – East Bank fault; PHBL – Prune Hill/Blue Lake fault; LL – Lacamas Lake fault. Inset: PB – Portland basin; TB – Tualatin basin.

3.2.3 Mid-Miocene to late Eocene (~17-35 Ma)

The pre-CRBG mid-Miocene to late Eocene (~17-35 Ma) isochore map reveals one distinct depocenter coincident with the western edge of the Tualatin basin (Figure 3.9). A gradual thinning of mid-Miocene to Eocene sedimentary rocks from the Tualatin basin eastward toward the Portland basin and western Cascades is observed. Maximum sediment thickness reaches ~17,060 ft (5.2 km) in the Tualatin basin and ~4,920 ft (1.5 km) in the Portland basin. We observe a minimum thickness of ~3,280 ft (1 km) in the core of the Dutch Canyon anticline (Figure 3.9). Uncertainty exists in the southern portion of the Portland basin, and is denoted by a cross-hatch pattern (Figure 3.9).

An area of local thickening coincident with the Portland Hills is bound by the Sylvan-Oatfield and Portland Hills faults. In this area, sediment thickness ranges from ~4,921-5,905 ft (1.5-1.8 km) and decreases to a thickness of ~2,952-3,937 ft (0.9-1.2 km) on its flanks (Figure 3.9). The East Bank fault shows a local thickening of sedimentary rock to the northeast that thins toward the northeast as it approaches the foothills of the western Cascades. On the southwest portion of the map (Figure 3.9), thickness of this unit changes variably across the Beaverton fault, suggesting that basement uplift in the southern domain is greater than elsewhere along its trace. The only observed change in thickness across the Canby-Molalla fault occurs near the normal segment of its mapped trace (Figure 3.9), though this transition is not as sharp or linear as other thickness breaks adjacent to faults in the map area.

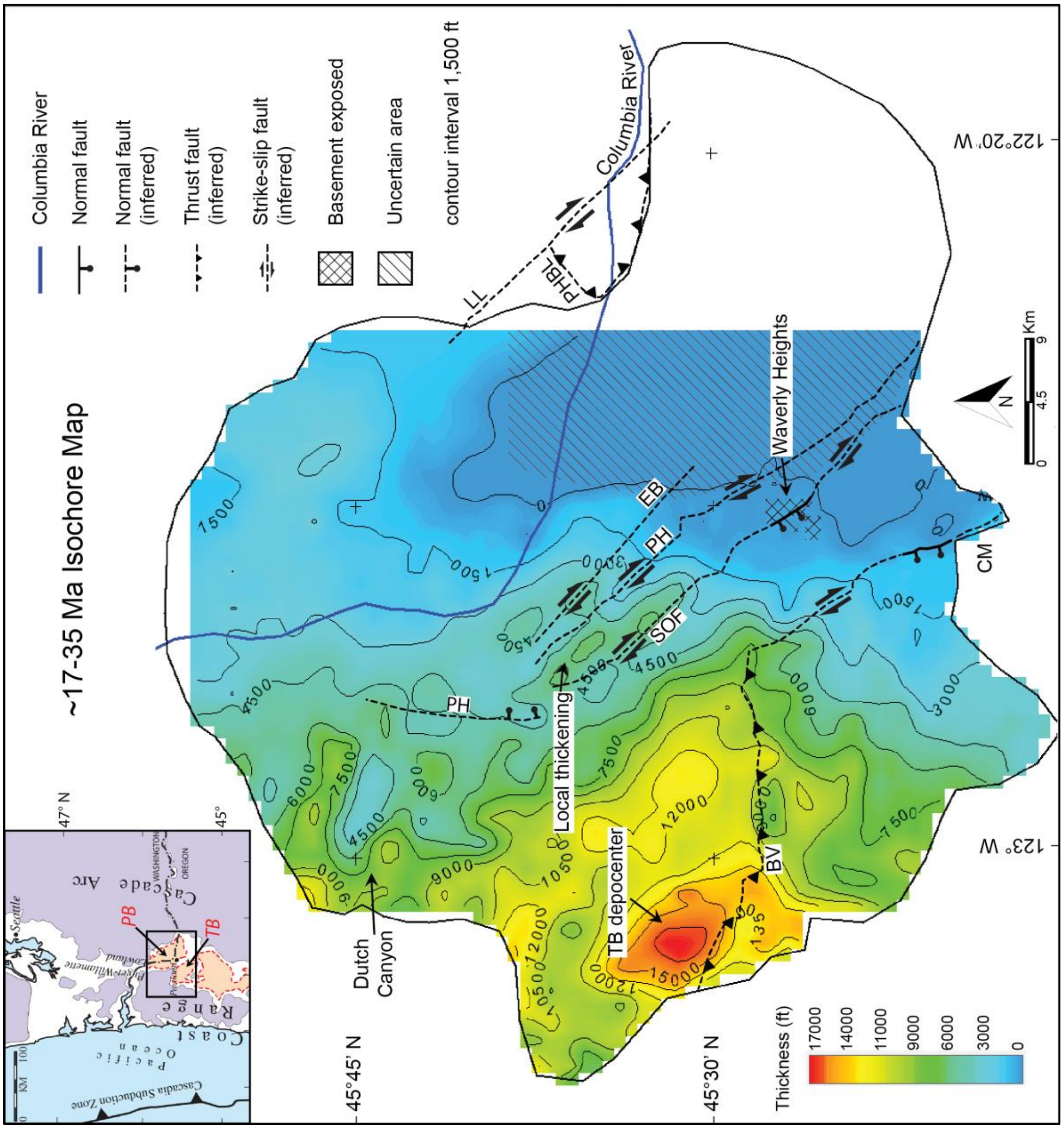

Figure 3.9. Mid-Miocene to late Eocene (~17-35 Ma) isochore map generated as the difference between the base CRBG and Eocene basement structure maps. Thickness packages less than ~1 km diameter are likely an interpolation artifact. Contour interval: 1,500 ft. Location of the Columbia River shown for reference. BV – Beaverton fault; CM – Canby-Molalla fault; SOF – Sylvan-Oatfield fault; PH – Portland Hills fault; EB – East Bank fault; PHBL – Prune Hill/Blue Lake fault; LL – Lacamas Lake fault. Inset: PB – Portland basin; TB – Tualatin basin.

CHAPTER 4: DISCUSSION

The evolution of the Cascade forearc is reflected in the Portland and Tualatin basins. Results show that Portland and Tualatin basin depocenters have shifted over time. This migration reflects a transition from Paleogene transtension to Neogene transpression in the forearc of Northwest Oregon, associated with the northward migration and clockwise rotation of the forearc over Cenozoic time (Wells and McCaffrey, 2013).

4.1 The Paleogene

A cross-section through the Portland and Tualatin basins that incorporates the gravity-derived basement surface from McPhee et al. (2014) suggests substantial downfaulting of Eocene basement prior to emplacement of CRBG in the mid-Miocene on faults still active today (Figure 4.1). I calculate a minimum vertical (normal) slip rate of ~0.04 mm/yr on the Sylvan-Oatfield and Portland Hills faults from the late Eocene to mid-Miocene (Figure 4.2), consistent with vertical slip rates on other faults in the region (Wong et al., 2000). Previous authors suggest that deformation on many faults in the study area is primarily strike-slip (Beeson et al., 1985, 1989a; Beeson and Tolan, 1990; Yelin and Patton, 1991; Blakely et al., 2000, 2004). Significant changes in basement elevation are reflected by both depositional thinning near Waverly Heights and erosional thinning near Dutch Canyon (Figure 3.9). Northwest-southeast directed extension in the central Oregon Coast Range started soon after accretion of the Siletz terrane, and was marked by normal faulting and northeast trending dike swarms (prior to rotation) that erupted the Tillamook Volcanics (Snavely and Wells, 1991, 1996; Wells et al., 2014).

McPhee et al. (2014) suggests that the Paleogene Tualatin basin initiated as a releasing-bend step-over between the Gales Creek and Portland Hills faults, creating accommodation space prior to CRBG emplacement (Cunningham and Mann, 2007). However, there is evidence that the Tualatin basin marked the edge of the continental shelf during this time and was an inboard extension of the marine Astoria basin. During the Paleogene, both are dominated by marine sedimentary rocks and unit thicknesses do not change significantly across the Coast Range where these rocks are documented in hydrocarbon exploration wells and are now exposed in outcrop (Niem and Niem, 1985; Niem et al., 1992b, 1992a). Thus, thinning of the ~17-35 Ma isochore map to the west is likely due largely to erosion as opposed to onlap onto a structural high (Figure 3.9). I estimate an average sediment accumulation rate in the Tualatin basin of ~286 m/Ma from Paleogene to mid-Miocene time based on a thickness of ~5,300 m and age range of ~17-35 Ma. This is similar to sediment accumulation rates in the Astoria basin during Oligocene (~275 m/Ma), estimated from well log data (Niem and Niem, 1985). These sediment accumulation rates are within the range of typical of marine basins at convergent boundaries (trench fill) (Schwab, 1976).

The thickest Paleogene sedimentary rocks (>5 km thick) in the Tualatin basin are coincident with a -44 mGal gravity low over basement offsets on the Gales Creek and Beaverton faults (Figure 4.1) (McPhee et al., 2014). A blind fault may control thinning of Paleogene to early Miocene sedimentary rocks under the west flank of the Portland Hills, though a lack of significant Holocene deformation limits potential fault activity to the Paleogene.

Portland basin sediments thin eastward onto the Paleogene coastline, which was near the western Cascades at that time (Figures 3.9, 4.1) (Niem et al., 1992b; Retallack et al., 2004; Evarts et al., 2009). The interfingering of marine sedimentary rock with incipient Cascade volcanics suggest deposition prior to the emergence of a subaerial Coast Range at ~20 Ma (Armentrout, 1983; McKeel, 1984; Stanley, 1991; Niem et al., 1992a; Snavely and Wells, 1996). An eastward shift of the Tualatin basin depocenter from the late Eocene to the mid-Miocene likely reflects uplift of the Coast Range, which resulted in the formation of an eastward-dipping homocline of Eocene to Oligocene marine strata prior to CRBG emplacement (Figures 3.8, 3.9) (Parker, 1990; Werner, 1990; Wells et al., 1994).

Cascade arc volcanism near its present location initiated ~45-40 Ma as a response to the outward stepping of the subduction zone due to the accretion of Siletzia to the continental margin (Snavely and Wells, 1996; Schmandt and Humphreys, 2011). Trehu et al. (1994) suggest that the western Cascades erupted over a well-developed sedimentary basin and that the eastern boundary of Siletzia occurs beneath the western Cascades. My Eocene basement map shows the Paleogene basin depocenter was >100 km to the west of the modern Cascade arc, with basement elevations increasing to the east toward the arc (Figures 3.9, 4.1). This interpretation is consistent with Evarts et al. (2009), who suggest that Paleogene and early Miocene sedimentary rocks interfingered with western Cascade volcanics prior to CRBG emplacement at the Paleogene coastline coincident with the Portland basin (Figure 4.1).

A -28 mGal gravity low centered over the Portland Hills coincides with 1.5-1.8 km of Paleogene and early Miocene sedimentary rocks bound by the dextral Sylvan-Oatfield and Portland Hills faults (Figure 3.9). Normal deformation on these steeply dipping (~70°) dextral faults offsets the basement surface, creating a graben into which a thicker package of Paleogene and early Miocene sediments were deposited (Panel C, Figure 4.2). This interpretation is tied to the Barber #1 exploration well, located in the Portland Hills, which penetrates ~2.1 km of volcanic rock, agglomerate, and sands (Figure 4.2) (Newton, 1969). Faulting likely continued during episodic Paleogene north-northwest extension, consistent with Eocene normal faulting in the Mist gas field (Niem and Niem, 1985) and eruption of upper middle and upper Eocene tholeiitic and alkalic basalts where the Coast Range is today (e.g., Tillamook Highlands) and offshore (Snavely and Wells, 1991, 1996; Snavely et al., 1993; Wells et al., 1994). Rift flank uplift resulted in up to ~1.2 km of relief along the northeast margin of the Tualatin basin and southwest margin of the nascent Portland basin (Figures 3.6, 4.1, 4.2).

Figure 4.1. (*on following page*). Geologic cross section A-A''' including all modeled units down to Eocene basement. Basement offsets (solid line) are interpreted from the residual gravity data (dotted line) of McPhee et al. (2014). Data constraints: 1 – WASH 206 (ID# 2206); 2 – WASH 633 (ID#2207); 3 – Interpolation guide (ID# 2201); 4 – Pick from Portland basin seismic profiles of Liberty (2002) (ID# 1667) (Supplemental Data Table 1). Vertical exaggeration 5:1. Inset: Top CRBG structure map with cross section line oriented NE-SW across the study area, location shown in Figure 3.4. Fault acronyms follow Figure 1.1.

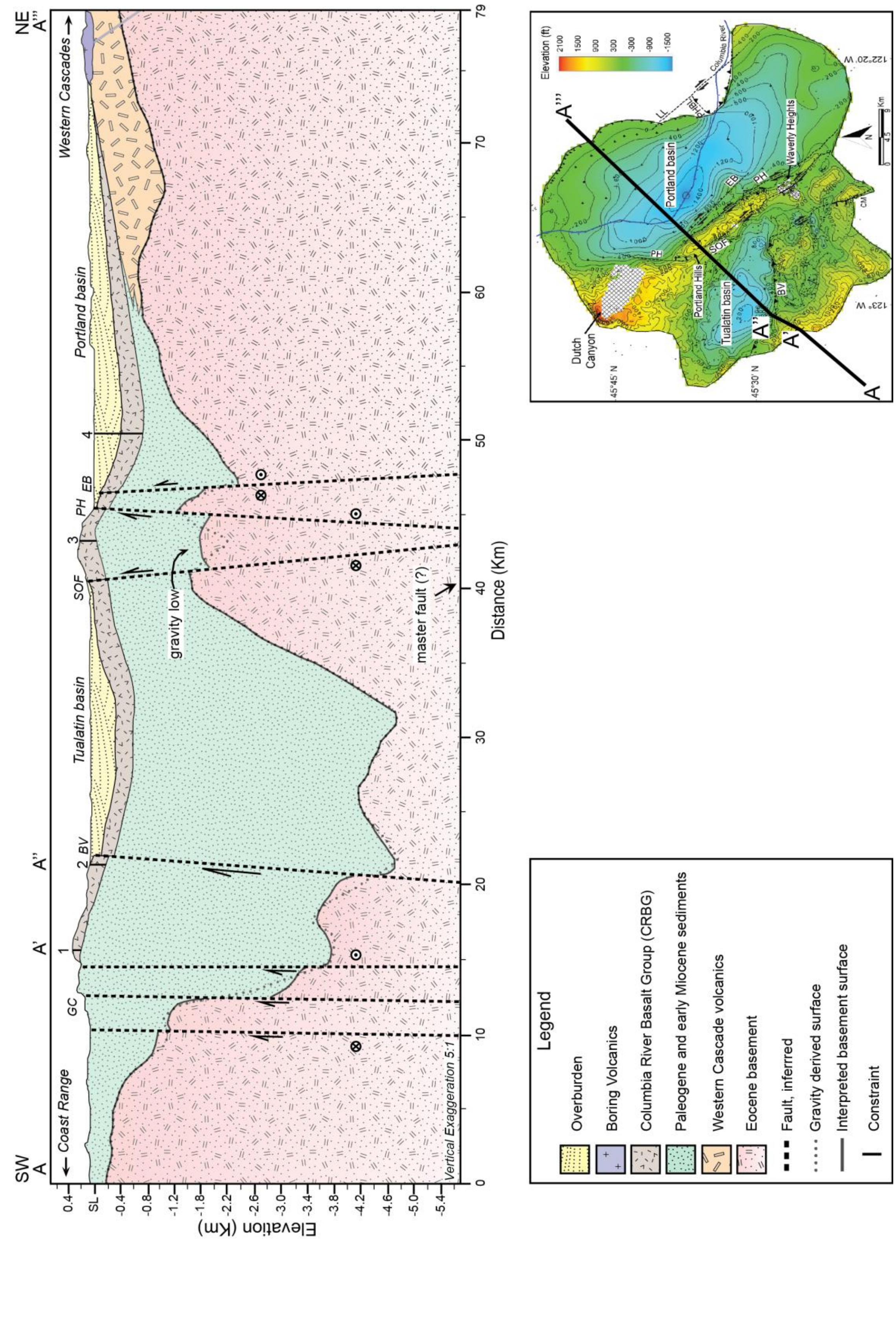

SW A
NE A'''
A'
A''
Coast Range
Tualatin basin
Portland basin
Western Cascades
GC
BV
SOF
PH
EB
gravity low
master fault (?)
Vertical Exaggeration 5:1
Elevation (Km)
Distance (Km)
Legend
Overburden
Boring Volcanics
Columbia River Basalt Group (CRBG)
Paleogene and early Miocene sediments
Western Cascade volcanics
Eocene basement
Fault, inferrred
Gravity derived surface
Interpreted basement surface
Constraint
Elevation (ft)
Dutch Canyon
Portland Hills
Portland basin
Tualatin basin
Waverly Heights
Columbia River
45°45' N
45°30' N
123° W
122°20' W

4.2 The Neogene

4.2.1 Columbia River flood basalts

Middle Miocene flood basalts of the CRBG inundated the Portland and Tualatin basins through the Cascades via the ancestral Columbia River at ~16.5 Ma (Beeson et al., 1989a; Beeson and Tolan, 1990; Reidel et al., 2013; Wells et al., 2018). Wide variation in flow thickness is evident in my CRBG (15.5-16.5 Ma) isochore map (Figure 3.8), indicating that there was significant variation in pre-existing topography. Encroaching flows deposited onto the Eocene basalt of Waverly Heights, incipient western Cascade arc, Goble Volcanics, Dutch Canyon anticline, and Paleogene to early Miocene sediments (Figures 3.8, 4.1) (Beeson et al., 1989a, 1989b). My mapping shows that flow paths were influenced by the major northwest-striking faults zones that dominate the study area (Anderson et al., 2013; Reidel et al., 2013). Previous workers have suggested that an incipient Portland Hills anticline diverted the earliest Grande Ronde Basalt flows of the CRBG (R_1/N_1 magnetic polarity; Figure A1), limiting their extent to the Portland basin (Beeson et al., 1989a; Evarts et al., 2009). However, the discovery of Downey Gulch and China Creek flows of the Grande Ronde Basalt (N_1 magnetic polarity; Figure A1) in the Tualatin basin suggests these earliest flows inundated the Tualatin basin as well (Dinterman and Duval, 2009; Wells et al., 2018). My CRBG isochore map and well data that bottom in R_2 Wapshilla Ridge in the Portland basin (MULT 106000) and older N_1 China Creek Member (WASH 55816) flows in the Portland basin suggest they were still connected at ~16.5 Ma (Figure 3.8) (Supplemental Data Table 1).

CRBG flows thin ~195-295 ft (60-90 m) across the flanks of a graben coinciding with the present-day location of the Portland Hills. Within the graben, flows reach thicknesses of up to ~787-984 ft (240-300 m) (Figures 3.8, 4.2). These thickness estimates are reasonably constrained by both well and outcrop data (Supplemental Data Table 1). Exposed Paleogene and early Miocene (pre-CRBG) sediments along the northeastern margin of the Tualatin basin along the Portland Hills suggest either a thinning of CRBG flows, post-emplacement erosion, or some combination of the two (see Panel A, Figure 4.1) (Wells et al., 2018). Walsh et al. (2011) interpret flows of both Grouse Creek and Wapshilla Ridge underneath the Portland Hills. Well data in the Tualatin basin penetrates R_2 Wapshilla Ridge and older N_1 China Creek Member flows, and R_2 Wapshilla Ridge flows in the Portland basin, suggesting that thinning is in part caused by erosion (USGS CRBG Database, Table A1). Gravity data and interpretive cross sections suggest that flows thinned depositionally onto gravity highs associated with the Eocene basalt of Waverly Heights and the Dutch Canyon anticline prior to inundating the Tualatin basin (Figure 3.9) (Beeson et al., 1989b; McPhee et al., 2014). South of the Portland basin, flows continued into the Northern Willamette basin, where the minimum elevation to top of CRBG is documented at < -1,640 ft (-500 m) along its main synclinal axis (Werner, 1990). Later flows encountered less topography as earlier flows filled in pre-existing lows, which is reflected in the widespread distribution of ~15.5 Ma Sentinel Bluffs flows of the Grande Ronde Basalt during N_2 time (Beeson et al., 1989a) (see Appendix, Figure A1).

4.2.2. Post-CRBG Structural Inversion

My data suggests that faults in the Portland and Tualatin basins were structurally inverted in the middle to late Miocene due to a change from transtension to transpression in the forearc. A shift to oblique convergence between the Farallon and North American plates since ~35 Ma has produced a broad distribution of plate boundary deformation (Engebretson et al., 1985), breaking the forearc up into a series of clockwise rotating blocks (Wells et al., 1998; Wells and McCaffrey, 2013; Savage and Wells, 2015). Clockwise rotation and northward migration of the forearc, as determined by GPS velocities and paleomagnetism has been occurring throughout much of the Cenozoic (McCaffrey et al., 2007). However, sometime in the mid to late Miocene, a local change in the regional stress field from transtensional to transpressive stress occurred. The dextral Sylvan-Oatfield and Portland Hills faults, which bound a Paleogene to early Miocene(?) graben under the present-day Portland Hills, provided planes of weakness exploited by transpressive stress in the mid to late Miocene resulting in structural inversion (Figure 4.2) (e.g. Letouzey et al., 1990). I calculate a minimum vertical slip rate of ~0.004 mm/yr on the Portland Hills fault and ~0.015 mm/yr on the Sylvan-Oatfield fault from the mid-Miocene to modern (Figure 4.2). The latter vertical slip rate is consistent with the 0.01-0.02 mm/yr calculated by Walsh et al. (2011) on the west Sylvan-Oatfield fault. My CRBG isochore map shows that inversion did not occur until sometime after CRBG was deposited (< 15 Ma), as CRBG thickens at the present-day location of the Portland Hills (Figure 3.8). The initiation of shortening during the mid-late Miocene is also documented in accelerated uplift of the Washington Cascades (Reiners et al., 2002), north-south shortening along the Seattle fault (ten Brink et al., 2002), and across the Yakima fold and thrust belt (McCaffrey et al., 2016). Late Miocene and Pliocene transpression in the Portland and Tualatin basins is consistent with regional aeromagnetic data that suggests the Sylvan-Oatfield and East Bank faults are steeply dipping structures that exhibit reverse slip (Blakely et al., 1995). Our interpretation of structural inversion of the Portland Hills is consistent with Beeson et al., 1989a, who interpreted the Portland Hills as a flower structure created by transpressive stress.

The east-west trending Beaverton fault in the southern Tualatin basin also shows evidence of structural inversion in the mid to late Miocene. Cooper Mountain, a post-CRBG fold with an east-west trending axis in the hanging wall of the Beaverton fault shows stratigraphic offset on the top CRBG surface consistent with reverse deformation on a fault dipping to the south (Figure 3.2). However, my CRBG isochore map shows that CRBG is relatively thick in the hanging wall, suggesting it was a normal fault in the mid-Miocene (Figure 3.8). McPhee et al. (2014) has also suggested that the Beaverton fault is an inversion structure that formed as a normal fault due to north-northwest extension in the Paleogene. My Eocene structure map shows up to ~4,921 ft (1.5 km) of basement offset on the Beaverton fault, consistent with the > 1 km estimation made by McPhee et al. (2014) (Figures 3.6, 3.9). Other east-west striking folds in the area (i.e., Parrett Mountain and the Chehalem Mountain uplift) also formed in response to north-south shortening (Beeson and Tolan, 1990). Structural inversion in the Tualatin and Portland basins is also consistent with the history of deformation on the Oregon shelf where normal faults were reactivated as thrust faults during late mid-Miocene transpression (Snavely and Wells, 1996). Previous workers have documented northeast-trending folds and faults being overprinted by Neogene north-northwest trending folds and faults in Oregon (Wells et al., 1983, 1994; Niem and Niem, 1985; Snavely and Wells, 1991, 1996; Snavely et al., 1993), providing widespread evidence of a major change in the stress regime from transtension in the Paleogene to transpression in the Neogene. This change is likely due to an increasing obliquity of convergence between the Farallon plate and North America, resulting in distributed dextral shear on faults across the forearc and northwest-directed extension in the Basin and Range (Engebretson et al., 1985; Wells and Heller, 1988; Wells and McCaffrey, 2013).

The location of distinct mid-Miocene to Pleistocene depocenters in the Portland and Tualatin basins suggests they were effectively separated by the Portland Hills during this time (Figures 3.2, 3.7). It is likely that basin separation was synchronous with structural inversion in the mid-late Miocene. The location of the Portland basin depocenter during the late Neogene suggests that the East Bank fault is exerting local control on accommodation space. My 0-15 Ma isochore map shows that post-CRBG basin fill in the Portland basin is ~55 m thicker than in the Tualatin basin, providing further evidence that uplift of the Oregon Coast Range has progressively pushed the forearc basin depocenter eastward through the Neogene (Figure 3.7). In the Puget Sound to the north, where lateral separation between the accretionary wedge (Olympics) and magmatic arc (Cascades) is greater, the Seattle basin reaches a maximum depth of ~9 km, nearly ~3 km deeper than the Tualatin basin (Johnson et al., 1994; Symons and Crosson, 1997; Rau and Johnson, 1999; Blakely et al., 2002; ten Brink et al., 2002; McPhee et al., 2014). Most of this difference is due to Neogene (20 Ma to modern) sedimentary rocks in the Seattle basin, which are significantly thicker than contemporaneous rocks in the Portland basin (~3.6 km thick versus ~500 m thick respectively) (Johnson et al., 1994) (Figure 3.7). This suggests that the location of Siletzia and accretionary wedge (Oregon

Coast Range and Olympic Mountains) uplift during the Neogene has exerted a first-order control on forearc accommodation space since the Miocene, not only in the Portland and Tualatin basins, but across the entire Cascadia forearc.

Average sediment accumulation rates across 0-15 Ma strata in the Portland and Tualatin basins are ~30 m/Ma, consistent with late Miocene to late Pliocene rates for the Tualatin basin estimated by Wilson (1997). This is an order of magnitude less than sediment accumulation rates estimated for Paleogene to early Miocene strata (see section 4.1 The Paleogene) and is consistent with the forearc's transition from a marine basin in an environment of extension to a continental forearc basin characterized by shortening. Neogene uplift of the Coast Range and a shift from transtensional to transpressive deformation in the mid-late Miocene set the stage for deformation observed today in the Portland and Tualatin basins, as the forearc continues to collide with the rigid Canadian Coast Mountains to the north (Snavely and Wells, 1996; Wilson, 1997; Wells et al., 1998; Wells and Simpson, 2001; McCaffrey et al., 2007; Wells and McCaffrey, 2013).

Figure 4.2. (*on following page*). Schematic cross section B-B' depicting mid-late Miocene structural inversion of the Portland Hills uplift. Prior to Columbia River Basalt Group (CRBG) deposition, normal faulting on the Sylvan-Oatfield and Portland Hills faults resulted in a graben with uplifted flanks on either side relative to the nascent Portland and Tualatin basins **(Panel C)**. Localized normal faulting continued up until the time of CRBG deposition, resulting in pre-existing topography **(Panel B).** This topography played an important role in controlling CRBG flow emplacement, where basalt flows are thicker in topographic lows and thinner on relative highs (Beeson et al., 1989). Post-CRBG emplacement, normal faults were reactivated as high angle reverse faults, resulting in the Portland Hills uplift **(Panel A)**. Structural inversion was likely in response to the steady clockwise rotation and northward migration of the Cascadia forearc (Wells and McCaffrey, 2013). The location of the Barber #1 exploration well constrains the thickness of Paleogene to early Miocene sedimentary rocks under the Portland Hills and is shown as a black solid line. Bedding orientations based on field mapping are depicted as tadpole with dip value (Wells et al., 2018). Depth to basement is from McPhee et al. (2014), derived from inversion of gravity data. No vertical exaggeration. SL = Sea Level. Inset map shows cross-section profile extending ~10 km northeast across the Portland Hills.

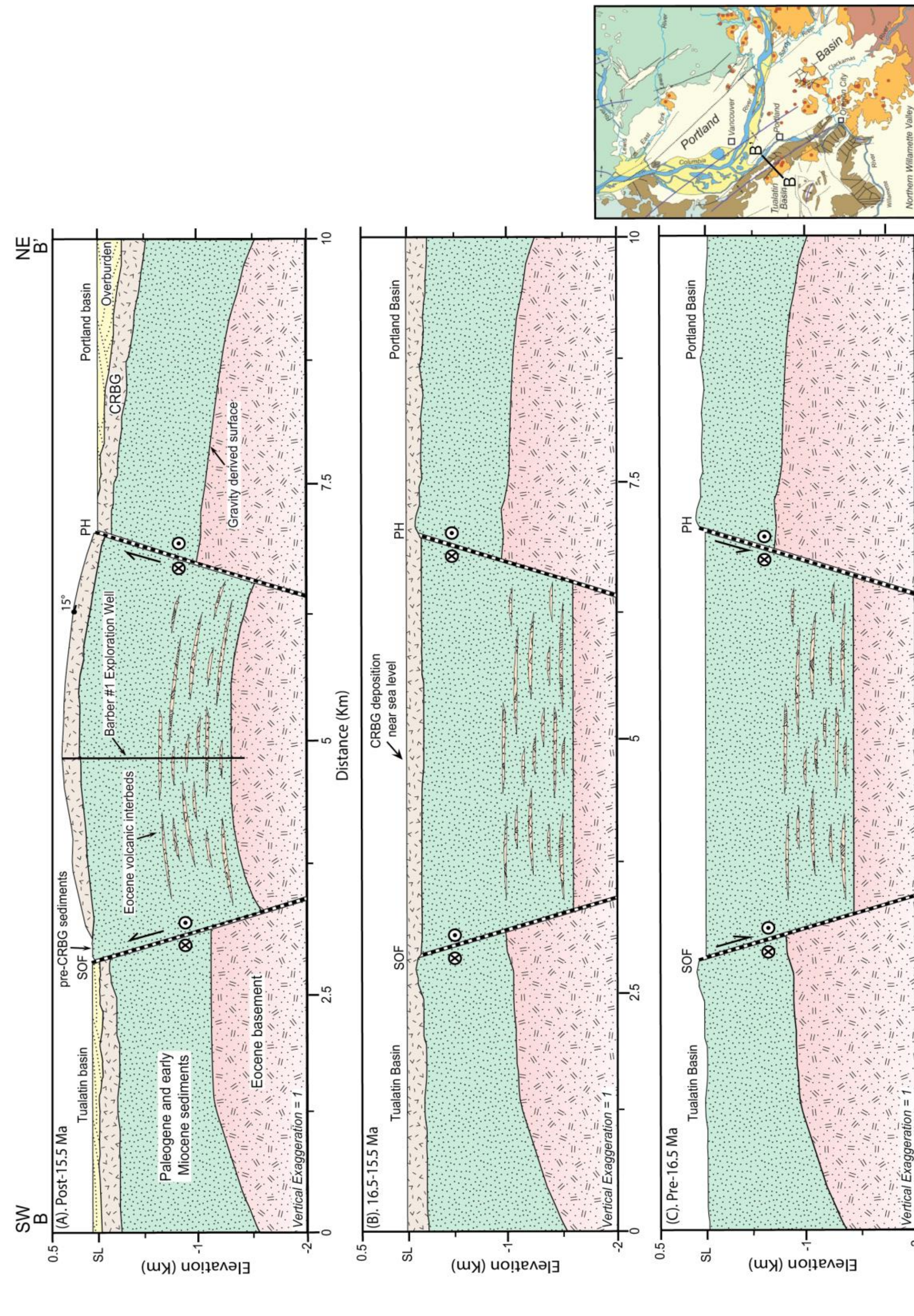
SW
B
NE
B'
(A). Post-15.5 Ma
Tualatin basin
pre-CRBG sediments
SOF
Eocene volcanic interbeds
Barber #1 Exploration Well
15°
PH
Gravity derived surface
CRBG
Overburden
Portland basin
Paleogene and early Miocene sediments
Eocene basement
Vertical Exaggeration = 1
Elevation (Km)
Distance (Km)
(B). 16.5-15.5 Ma
CRBG deposition near sea level
Tualatin Basin
Portland Basin
(C). Pre-16.5 Ma
Portland
Basin
Vancouver
Oregon City
Clackamas
Columbia
Northern Willamette Valley

CHAPTER 5: CONCLUSIONS AND FUTURE WORK

Although the Portland basin is separated from the Tualatin basin by the Portland Hills, inversion of gravity data suggests that the two were connected as one continuous basin sometime prior to CRBG deposition. An eastward shift of the forearc basin depocenter over the Neogene likely reflects uplift of the Coast Range to the west. Local thickening of CRBG flows over a gravity low coincident with the Portland Hills suggests that Neogene transpression in the forearc reactivated the Sylvan-Oatfield and Portland Hills faults as dextral reverse faults. This structure separated the once continuous Portland and Tualatin basins in the mid-late Miocene. Structural inversion was the result of a change from transtension to transpression in the Oregon Cascades forearc. This change in regional stress, along with uplift of the Oregon Coast Range, caused a 10-fold decrease in sediment accumulation rates across the Portland and Tualatin basins. Transpressional oblique-slip faulting continues to play a role in deforming the region as the forearc undergoes clockwise rotation and collides with the rigid Canadian Coast Mountains to the north, creating evident hazard for the Portland metropolitan and surrounding areas.

To better understand the forcing behind Cascade forearc basin formation, a flexural model may be used to elucidate the relative roles of the western Cascades and Coast Range acting as a load on the lithosphere (e.g. Waltham et al., 2008; Allen and Allen, 2013). In addition, re-processing regional aeromagnetic data could further delineate unit boundaries leading to a better understanding of subsurface structure, including shallow CRBG in both the Portland and Tualatin basins (Blakely and Simpson, 1986; Blakely et al., 2000).

REFERENCES

Allen, P.A., and Allen, J.R., 2013, Basin Analysis: Principles and Application to Petroleum Play Assessment: West Sussex, Wiley & Blackwell, 602 p.

Anderson, E.M., 1963, The Dyamics of Faulting and Dyke Formation with Applications to Britain: Edinburgh, Oliver and Boyd, 206 p.

Anderson, E.M., 1905, The dynamics of faulting: Transactions of the Edinburgh Geological Society, v. 8, p. 387–402.

Anderson, J.L., Tolan, T.L., and Wells, R.E., 2013, Strike-slip faults in the western Columbia River flood basalt province, Oregon and Washington, *in* The Columbia River Basalt Province: Geological Society of America Special Paper 497, p. 325–347.

Armentrout, J.M., 1983, Correlation of Cenozoic Stratigraphic Units of Western Oregon and Washington: Oregon Department of Geology and Mineral Industries Oil and Gas Investigations 7, p. 93.

Bassett, D., and Watts, A.B., 2015, Gravity anomalies, crustal structure, and seismicity at subduction zones: 2. Interrelationship between fore-arc structure and seismogenic behavior: AGU Publications - Geochemistry, Geophysics, Geosystems, v. 16, p. 1541–1576, doi:10.1002/2014GC005685.

Beeson, M.H., Fecht, K.R., Reidel, S.P., and Tolan, T.L., 1985, Regional correlations within the Frenchman Springs Member of the Columbia River Basalt Group: New insights into the middle Miocene tectonics of northwestern Oregon: Oregon Geology, v. 47, p. 86–99, doi:10.1016/j.jvc.2009.09.003.

Beeson, M.H., and Tolan, T.L., 1990, The Columbia River Basalt Group in the Cascade Range: A Middle Miocene reference datum for structural analysis: Journal of Geophysical Research, v. 95, p. 12.

Beeson, M.H., Tolan, T.L., and Anderson, J.L., 1989a, The Columbia River Basalt Group in western Oregon: Geologic structures and other factors that controlled flow emplacement patterns, *in* Volcanism and tectonism in the Columbia River flood-basalt province: Geological Society of America, Special Paper 239, p. 223–246.

Beeson, M.H., Tolan, T.L., and Madin, I.P., 1989b, Geologic map of the Lake Oswego quadrangle, Clackamas, Multnomah, and Washington Counties, Oregon, Oregon Department of Geology and Mineral Industries Geological Map Series GMS-59, scale 1:24,000.: State of Oregon Department of Geology and Mineral Industries GMS-59, p. 1.

Blakely, R.J., Beeson, M.H., Cruikshank, K., Wells, R.E., Johnson, A., and Walsh, K., 2004, Gravity study through the Tualatin Mountains, Oregon: Understanding crustal structure and earthquake hazards in the Portland urban area: Bulletin of the Seismological Society of America, v. 94, p. 1402–1409, doi:10.1785/012003045.

Blakely, R.J., and Simpson, R.W., 1986, Approximating edges of source bodies from magnetic or gravity anomalies: Geophysics, v. 51, p. 1494–1498.

Blakely, R.J., Wells, R.E., Tolan, T.L., Beeson, M.H., Trehu, A.M., and Liberty, L.M., 2000, New aeromagnetic data reveal large strike-slip (?) faults inthe Northern Willamette Valley, Oregon: Bulletin of the Geological Society of America, v. 112, p. 1225–1233, doi:10.1130/0016-7606(2000)112<1225:NADRLS>2.0.CO;2.

Blakely, R.J., Wells, R.E., Weaver, C.S., and Johnson, S.Y., 2002, Location, structure, and seismicity of the Seattle fault zone, Washington: Evidence from aeromagnetic anomalies, geologic mapping, and seismic-reflection data: Geological Society of America Bulletin, v. 114, p. 169–177.

Blakely, R.J., Wells, R.E., Yelin, T.S., Madin, I.P., and Beeson, M.H., 1995, Tectonic setting of the portland - Vancouver area, Oregon and Washington - constraints from low-altitude aeromagnetic data: Geological Society of America Bulletin, v. 107, p. 1051–1062.

ten Brink, U.S., Molzer, P.C., Fisher, M.A., Blakely, R.J., Bucknam, R.C., Parsons, T., Crosson, R.S., and Creager, K.C., 2002, Subsurface Geometry and Evolution of the Seattle Fault Zone and the Seattle Basin, Washington: Bulletin of the Seismological Society of America, v. 92, p. 1737–1753.

Burns, E.R., Morgan, D.S., Peavler, R.S., and Kahle, S.C., 2011, Three-Dimensional Model of the Geologic Framework for the Columbia Plateau Regional Aquifer System , Idaho , Oregon , and Washington: U.S. Geological Survey Scientific Investigations Report 2010-5246, p. 44, http://pubs.usgs.gov/sir/2010/5246.

Conrey, R.M., Sherrod, D.R., Uto, K., and Uchiumi, S., 1996, Potassium-Argon Ages from Mount Hood Area of Cascade Range, Northern Oregon: ISOCHRON/WEST, v. 63, p. 10–20.

Cunningham, W.D., and Mann, P., 2007, Tectonics of strike-slip restraining and releasing bends: Geological Society, London, Special Publications 290, p. 1–12.

Dinterman, P., and Duval, A., 2009, Preliminary geologic map of the Buxton 7.5' quadrangle, Washington County, Oregon: U.S. Geological Survey Open-File Report 2009-1186, scale 1:24,000, http://pubs.usgs.gov/of/2009/1186/.

Duncan, R.A., 1982, A captured island chain in the coast range of Oregon and Washington: Journal of Geophysical Research: Solid Earth, v. 87, p. 827–837.

Engebretson, D.C., Cox, A., and Gordon, R.G., 1985, Relative Motions Between Oceanic and Continental Plates in the Pacific Basin: Geological Society of America Special Paper 206, p. 65.

Evarts, R.C., 2006, Geologic map of the Lacamas Creek quadrangle, Clark County, Washington: U.S. Geological Survey Scientific Investigations Map 2924, scale 1:24,000, https://pubs.usgs.gov/sim/2006/2924/.

Evarts, R.C., 2004a, Geologic map of the Ridgefield quadrangle, Clarck and Cowlitz Counties, Washington: U.S. Geological Survey Scientific Investigations Map 2844, scale: 1:24,000, https://pubs.usgs.gov/sim/2004/2844/.

Evarts, R.C., 2004b, Geologic Map of the Saint Helens Quadrangle, Columbia County, Oregon, and Clark and Cowlitz Counties, Washington: U.S. Geological Survey Scientific Investigations Map 2834, scale: 1:24,000, http://pubs.er.usgs.gov/publication/sim2834.

Evarts, R.C., 2004c, Geologic Map of the Woodland Quadrangle, Clark and Cowlitz Counties, Washington: U.S. Geological Survey Scientific Investigations Map 2827, scale: 1:24,000, http://pubs.er.usgs.gov/publication/sim2827.

Evarts, R.C., Conrey, R.M., Fleck, R.J., and Hagstrum, J.T., 2010, The Boring Volcanic Field of the Portland-Vancouver area, Oregon and Washington: Tectonically anomalous forearc volcanism in an urban setting: The Geological Society of America Field Guide 15, p. 253–270, doi:10.1130/2009.fld015(13).

Evarts, R.C., O'Connor, J.E., Wells, R.E., and Madin, I.P., 2009, The Portland basin: A (big) river runs through it: GSA Today, v. 19, p. 7, doi:10.1130/GSATG58A.1.

Flemings, P.B., and Jordan, T.E., 1990, Stratigraphic modeling of foreland basins: Interpreting thrust deformation and lithosphere rheology: Geology, v. 18, p. 430–434.

Givler, R., Witter, R., Madin, I., and Amos, C., 2009, Paleoseismology of the Mount Angel fault in the Willamette Valley, Oregon: Collaborative research with William Lettis & Associates, Inc. and the Oregon Department of Geology and Mineral Industries: U.S. Geological Survey National Earthquake Hazards Reduction Program, p. 51.

Hammond, P.E., 1979, A Teconic Model for Evolution of the Cascade Range, *in* Pacific Coast Paleogeography Symposium 3: Cenozoic Paleogeography of the Western United States, p. 19.

Heller, P.L., Angevine, C.L., Winslow, N.S., and Paola, C., 1988, Two-phase stratigraphie model of foreland-basin sequences: Geology, v. 16, p. 501–504.

Horst, A., Streig, A.R., Wells, R.E., and Guilderson, T., 2019, Seismic Source Characterization of Faults in the Portland and Tualatin Basins and a Paleoseismic Study of the Gales Creek Fault, OR, *in* Geological Society of America Abstracts with Programs, Cordilleran Section, v. 51, no. 4, doi:10.1130/abs/2019CD-329221.

Ingersoll, R. V., 1978, Petrofacies and Petrologic Evolution of the Late Cretaceous Fore-

Arc Basin, Northern and Central California: The Journal of Geology, v. 86, p. 335–352.

Johnson, S.Y., Potter, C.J., and Armentrout, J.M., 1994, Origin and evolution of the Seattle fault and Seattle basin, Washington: Geology, v. 22, p. 71–74.

Letouzey, J., Werner, P., and Marty, A., 1990, Fault reactivation and structural inversion. Backarc and intraplate compressive deformations. Example of the eastern Sunda shelf (Indonesia): Tectonophysics, v. 183, p. 341–362.

Liberty, L.M., 2002, Procurement and reprocessing of an industry marine seismic reflection profile from the Columbia River , Oregon and Washington: Center for Geophysical Investigation of the Shallow Subsurface (CGISS), Boise State University, p. 1–14.

Liberty, L.M., Hemphill-Haley, M.A., and Madin, I.P., 2003, The Portland Hills Fault: Uncovering a hidden fault in Portland, Oregon using high-resolution geophysical methods: Tectonophysics, p. 89–103, doi:10.1016/S0040-1951(03)00152-5.

Madin, I.P., 1990, Earthquake-Hazard Geology Maps of the Portland Metropolitan area, Oregon: Text and Map Explanation: State of Oregon Department of Geology and Mineral Industries Open-File Report 0-90-2, p. 32.

McCaffrey, R., King, R.W., Wells, R.E., Lancaster, M., and Miller, M.M., 2016, Contemporary deformation in the Yakima fold and thrust belt estimated with GPS: Geophysical Journal International, p. 1–11.

McCaffrey, R., Qamar, A.I., King, R.W., Wells, R.E., Khazaradze, G., Williams, C.A., Stevens, C.W., Vollick, J.J., and Zwick, P.C., 2007, Fault locking, block rotation and crustal deformation in the Pacific Northwest: Geophysical Journal International, p. 1315–1340, doi:10.1111/j.1365-246X.2007.03371.x.

McCarthy, K.A., and Anderson, D.B., 1990, Ground-Water Data for the Portland Basin , Oregon and Washington: U.S. Geological Survey Open-File Report 90-126, p. 1–43.

McKeel, D.R., 1984, Biostratigraphy of Exploratory Wells in Western Coos, Douglas, and Lane Counties, Oregon: State of Oregon Department of Geology and Mineral Industries Oil and Gas Investigations 11, p. 24.

McPhee, D.K., Langenheim, V.E., Wells, R.E., and Blakely, R.J., 2014, Tectonic evolution of the tualatin basin, northwest Oregon, as revealed by inversion of gravity data: Geosphere, v. 10, p. 264–275, doi:10.1130/GES00929.1.

Newton, V.C., 1969, Subsurface Geology of the Lower Columbia and Willamette Basins, Oregon: State of Oregon Department of Geology and Mineral Industries Oil and Gas Investigations No. 2, p. 130.

Niem, A.R., MacLeod, N.S., Snavely, P.D., Huggins, D., Fortier, J.D., Meyer, J.H., Seeling, A.F., and Niem, W.A., 1992a, Onshore-offshore Geologic Cross Section, Northern Oregon Coast Range To Continental Slope: State of Oregon Department of Geology and Mineral Industries Special Paper 26, p. 1.

Niem, A.L., and Niem, W.A., 1985, Geologic Map of the Astoria Basin, Clatsop and Northernmost Tillamook Counties, Northwest Oregon: State of Oregon Department of Geology and Mineral Industries OGI-14, p. 1.

Niem, W.A., Niem, A.R., and Snavely, P.D., 1992b, Early and Mid-Tertiary oceanic realm and continental margin - western Washington-Oregon coastal sequence, *in* The Cordilleran Orogen: Conterminous U.S.: Geological Society of America The Geology of North America, volume G-3, p. 265–270.

Orzol, L.L., Wozniak, K.C., Meissner, T.R., and Lee, D.B., 2000, Ground-water and water-chemistry data for the Willamette basin, Oregon: U.S. Geological Survey Water-Resources Investigations Report 99-4036, p. 151.

Parker, M.J., 1990, The Oligocene and Miocene Geology of the Tillamook Embayment, Tillamook County, Northwest Oregon: Oregon State University M.S. thesis, p. 275.

Popowski, T.A., 1996, Geology, structure, and tectonic history of the Tualatin Basin, northwestern Oregon: Oregon State University M.S. thesis, p. 142.

Rau, W.W., and Johnson, S.Y., 1999, Well Stratigraphy and Correlations, Western Washington and Northwestern Oregon: U.S. Geological Survey Geologic Investigations Series I-2621, p. 1–36.

Redwine, J., Klinger, R.E., Piety, L.A., Wells, R.E., Sherrod, B.L., Howe, J.C., Levinson, R., Hornsby, K., and Niem, A., 2017, Quaternary Activity on the Gales Creek Fault, Northwest Oregon, *in* Geological Society of America, Abstracts with Programs, v. 49, no. 6, doi:10.1130/abs/2017AM-306019.

Reidel, S.P., Camp, V.E., Tolan, T.L., and Martin, B.S., 2013, The Columbia River flood basalt province: Stratigraphy, areal extent, volume, and physical volcanology, *in* The Columbia River Flood Basalt Province: Geological Society of America Special Paper 497, p. 1–43.

Reiners, P.W., Ehlers, T.A., Garver, J.I., Mitchell, S.G., Montgomery, D.R., Vance, J.A., and Nicolescu, S., 2002, Late Miocene exhumation and uplift of the Washington Cascade Range: Geology, v. 30, p. 767–770.

Retallack, G.J., Orr, W.N., Prothero, D.R., Duncan, R.A., Kester, P.R., and Ambers, C.P., 2004, Eocene-Oligocene extinction and paleoclimate change near Eugene, Oregon: Geological Society of America Bulletin, v. 116, p. 817–839.

Roe, W.P., and Madin, I.P., 2013, 3D Geology and Shear-Wave Velocity Models of the Portland , Oregon , Metropolitan Area: Oregon Department of Geology and Mineral Industries Open-File Report O-13-12, p. 52.

Rogers, G.C., 2002, The role of phase changes in the development of forearc basins, *in*

The Cascadia Subduction Zone and Related Subduction Systems: Seismic Structure, Intraslab Earthquakes and Processes, and Earthquake Hazards U.S. Geological Survey Open-File Report 02-328, p. 145.

Savage, J.C., and Wells, R.E., 2015, Identifying block structure in the Pacific Northwest, USA: Journal of Geophysical Research: Solid Earth, v. 2015, p. 450–487, doi:10.1002/2014JB011176.Received.

Schmandt, B., and Humphreys, E., 2011, Seismically imaged relict slab from the 55 Ma Siletzia accretion to the northwest United States: Geology, v. 39, p. 175–178.

Schwab, F.L., 1976, Modern and ancient sedimentary basins: Comparative accumulation rates: Geology, v. 4, p. 723–727.

Snavely, P.D., MacLeod, N.S., and Wagner, H.C., 1968, Tholeiitic and alkalic basalts of the Eocene Siletz River Volcanics, Oregon: American Journal of Science, v. 266, p. 454–481, doi:10.2475/ajs.266.6.454.

Snavely, P.D., and Wagner, H.C., 1963, Tertiary Geologic History of Western Oregon and Washington: State of Washington Department of Conservation, p. 32.

Snavely, P.D., and Wells, R.E., 1996, Cenozoic Evolution of the Continental Margin of Oregon and Washington, *in* Assessing Earthquake Hazards and Reducing Risk in the Pacific Northwest U.S. Geological Survey Professional Paper 1560, p. 161–182.

Snavely, P.D., and Wells, R.E., 1991, Cenozoic Evolution of the Continental Margin of Oregon and Washington, *in* Earthquake Hazards in the Pacific Northwest of the United States United States Department of the Interior Geological Survey Open-File Report 91-441-B, p. 1–39.

Snavely, P.D., Wells, R.E., and Minasian, D., 1993, The Cenozoic Geology of the Oregon and Washington Coast Range, *in* Northwest Petroleum Association 9th Annual Field Trip Cenozoic Geology of Coastal Northwest Oregon U.S. Geological Survey Open-File Report 93-189, v. Open-File, p. 1–40.

Spitzer, R., White, R.S., Christie, P.A.F., and Team, I., 2008, Seismic characterization of basalt flows from the Faroes margin and the Faroe-Shetland basin: Geophysical Prospecting, v. 56, p. 21–31.

Stanley, R.G., 1991, Geologic Basis for Petroleum Resource Assessment of Onshore Western Oregon and Washington (Province 72): U.S. Geological Survey Open-File Report 88-450X, p. 1–31.

Swanson, R.D., McFarland, W.D., Gonthier, J.B., and Wilkinson, J.M., 1993, A descritption of Hydrogeologic Units in the Portland Basin, Oregon and Washington: U.S. Geological Survey Water-Resources Investigations Report 90-4196, p. 64.

Symons, N.P., and Crosson, R.S., 1997, Seismic velocity structure of the Puget Sound region from 3-D non-linear tomography: Geophysical Research Letters, v. 24, p.

2593–2596.

Tacher, L., Pomian-Srzednicki, I., and Parriaux, A., 2006, Geological uncertainties associated with 3-D subsurface models: Computers and Geosciences, v. 32, p. 212–221, doi:10.1016/j.cageo.2005.06.010.

Thomas, G.C., Crosson, R.S., Carver, D.L., and Yelen, T.S., 1996, The 25 March 1993 Scot Mills, Oregon, Earthquake and Aftershock Sequence: Spatial Distribution, Focal Mechanisms, and the Mount Angel Fault: Bulletin of the Seismological Society of America, v. 86, p. 11.

Tolan, T.L., and Beeson, M.H., 1984, Intracanyon Flows of the Columbia River Basalt Group in the Lower Columbia River Gorge and Their Relationship To the Troutdale Formation: Bulletin of the Geological Society of America, v. 95, p. 463–477, doi:10.1130/0016-7606(1984)95<463:IFOTCR>2.0.CO;2.

Tolan, T.L., Martin, B.S., Reidel, S.P., Kauffman, J.D., Garwood, D.L., and Anderson, J.L., 2009, Stratigraphy and tectonics of the central and eastern portions of the Columbia River Flood-Basalt Province: An overview of our current state of knowledge, *in* Volcanoes to Vineyards: Geologic Field Trips through the Dynamic Landscape of the Pacific Northwest: Geological Society of America Field Guide 15, v. 15, p. 645–672.

Treasher, R.C., 1942, Geologic History of the Portland Area: Department of Geology and Mineral Industries GMI Short Paper No. 7, p. 18.

Trehu, A.M., Asudeh, I., Brocher, T.M., Luetgert, J.H., Mooney, W.D., Nabelek, J.L., and Nakamura, Y., 1994, Crustal architecture of the cascadia forearc: Science, v. 266, p. 237–243, doi:10.1126/science.266.5183.237.

Trimble, D.E., 1963, Geology of Portland, Oregon and Adjacent Areas: Geological Society of America Bulletin, v. 1119, p. 247.

Waitt, R.B., 1985, Case for periodic, colossal jökulhlaups from Pleistocene glacial Lake Missoula: Geological Society of America Bulletin, v. 96, p. 1271–1286.

Walker, G.W., and MacLeod, N.S., 1991, Geologic map of Oregon: U.S. Geological Survey, scale 1:500 000, p. 1.

Walsh, K., Peterson, G.L., Beeson, M.H., Wells, R.E., Fleck, R.J., Evarts, R.C., Duvall, A., Blakely, R.J., and Burns, S., 2011, A Tunnel Runs Through It - An Inside View of the Tualatin Mountains, Oregon: USGS Scientific Investigations Map 3144, p. 1.

Waltham, D., Hall, R., Smyth, H.R., and Ebinger, C.J., 2008, Basin formation by volcanic arc loading, *in* Formation and Applications of the Sedimentary Record in Arc Collision Zones: Geological Society of America Special Paper 436, p. 11–26.

Wells, R.E., Bukry, D., Friedman, R., Pyle, D., Duncan, R., Haeussler, P., and Wooden, J., 2014, Geologic history of Siletzia, a large igneous province in the Oregon and

Washington Coast Range: Correlation to the geomagnetic polarity time scale and implications for a long-lived Yellowstone hotspot: Geosphere, v. 10, p. 692–719, doi:10.1130/GES01018.1.

Wells, R.E., Haugerud, R., Niem, A., Niem, W., Ma, L., Madin, I., and Evarts, R., 2018, New Geologic Mapping of the Northwestern Willamette Valley, Oregon, and its American Viticultural Areas (AVAs)—A Foundation for Understanding Their Terroir: U.S. Geological Survey Open-File Report 2018-1044, p. 1, doi:10.3133/ofr20181044.

Wells, R.E., and Heller, P.L., 1988, The relative contribution of accretion, shear, and extension to Cenozoic tectonic rotation in the Pacific Northwest: Geological Society of America Bulletin, v. 100, p. 325–338.

Wells, R.E., and McCaffrey, R., 2013, Steady rotation of the Cascade arc: Geology, v. 41, p. 1027–1030, doi:10.1130/G34514.1.

Wells, R.E., Niem, A.R., MacLeod, N.S., Snavely, P.D., and Niem, W.A., 1983, Preliminary Geologic Map of the West Half of the Vancouver (WA.-ORE.) 1°x2° Quadrangle, Oregon: U.S. Geological Survey Open File Report 83-591, p. 1.

Wells, R.E., and Simpson, R.W., 2001, Northward migration of the Cascadia forearc in the northwestern U.S. and implications for subduction deformation: Earth, Planets, Space, v. 53, p. 275–283, doi:10.1186/BF03352384.

Wells, R.E., Snavely, P.D., MacLeod, N.S., Kelly, M.M., and Parker, M.J., 1994, Geologic map of the Tillamook Highlands, northwest Oregon Coast Range: U.S. Geological Survey Open-File Report 94-0021, p. 24, https://pubs.usgs.gov/of/1995/of95-670/.

Wells, R.E., Weaver, C.S., and Blakely, R.J., 1998, Fore-arc migration in Cascadia and its neotectonic significance: Geology, v. 26, p. 759–762, doi:10.1130/0091-7613(1998)026<0759:FAMICA>2.3.CO;2.

Werner, K.S., 1990, I, Direction of maximum horizontal compression in western Oregon determined by borehole breakouts: II, Structure and tectonics of the northern Willamette Valley, Oregon: Oregon State University M.S. thesis, p. 156.

Wilson, D.C., 1998, Post-middle Miocene geologic evolution of the Tualatin basin, Oregon: Oregon Geology, v. 60, p. 99–116.

Wilson, D.C., 1997, Post-Middle Miocene Geologic History of the Tualatin Basin, Oregon with Hydrogeologic Implications: Portland State University Ph.D. Dissertation, p. 310.

Wilson, D.C., and Peterson, M., 1996, Neogene sediment differences between the Tualatin and Portland basins, Oregon: A case for the existence of post-middle Miocene Tualatin highlands, *in* Geological Society of America Abstracts with

Programs, Cordilleran Section, p. 125.

Wong, I.G., Hemphill-Haley, M.A., Liberty, L.M., and Madin, I.P., 2001, The Portland Hills fault: An earthquake generator or just another old fault? Oregon Geology, v. 63.

Wong, I., Silva, W., Bott, J., Wright, D., Thomas, P., Gregor, N., Li, S., Mabey, M., Sojourner, A., and Wang, Y., 2000, Earthquake scenario and probabilistic ground shaking maps for the Portland, Oregon, metropolitan area: Oregon Department of Geology and Mineral Industries Interpretive Map Series 16 IMS-16, p. 11.

Yeats, R.S., Graven, E.P., Werner, K.S., Goldfinger, C., and Popowski, T.A., 1996, Tectonics of the Willamette Valley, Oregon, *in* Assessing Earthquake Hazards and Reducing Risk in the Pacific Northwest Volume 1 U.S. Geological Survey Professional Paper 1560, p. 183–222.

Yeats, R.S., Graven, E.P., Werner, K.S., Goldfinger, C., and Popowski, T., 1991, Tectonics of the Willamette Valley, Oregon, *in* Earthquake Hazards in the Pacific Northwest of the United States United States Department of the Interior Geological Survey Open-File Report 91-441-P, p. 1–47.

Yelin, T.S., and Patton, H.J., 1991, Seismotectonics of the Portland, Oregon, region: Bulletin of the Seismological Society of America, v. 81, p. 109–130.

Zak, I., and Freund, R., 1981, Asymmetry and basin migration in the dead sea rift: Tectonophysics, v. 80, p. 27–38.

APPENDIX

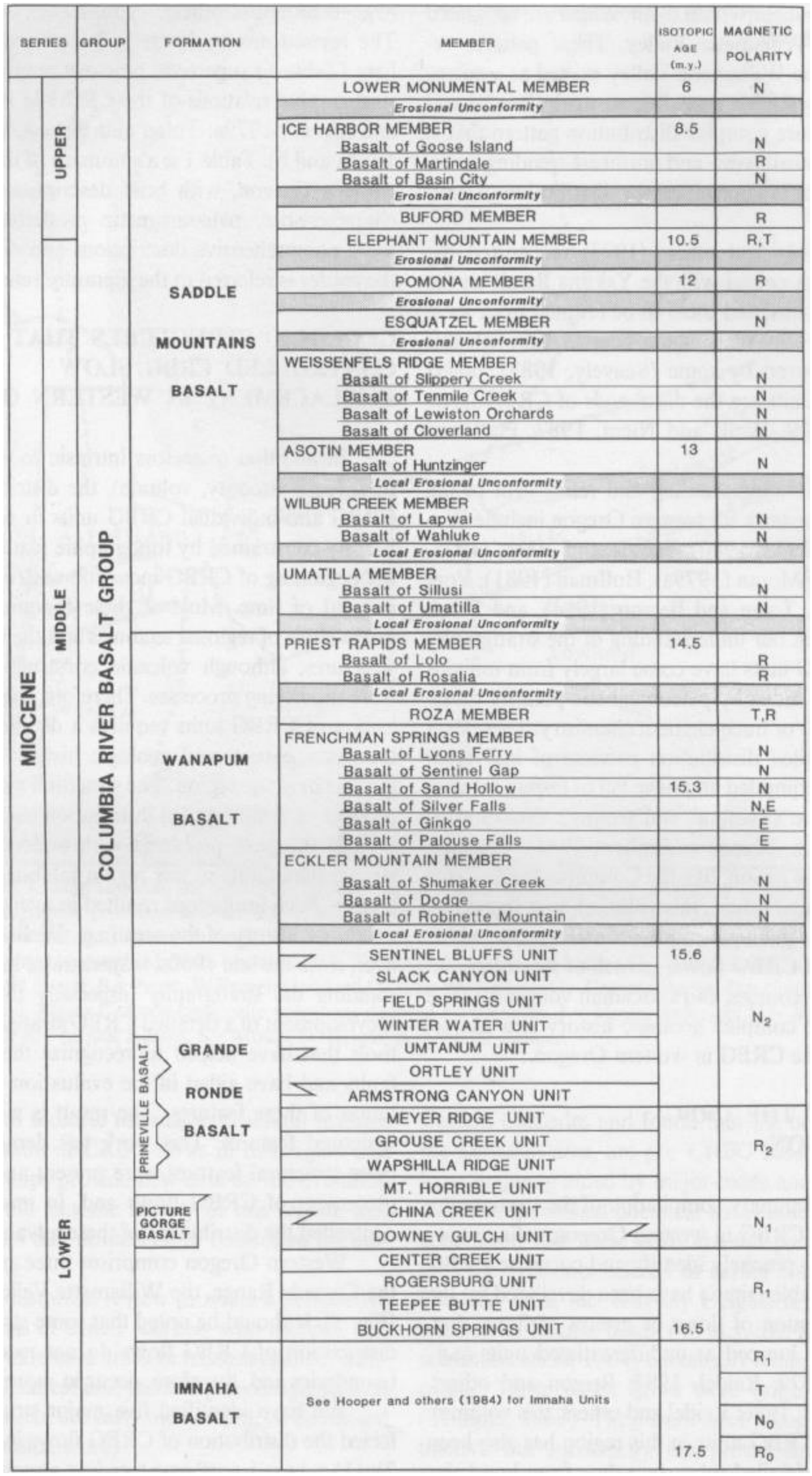

Figure A1. Stratigraphic column of CRBG. N = normal magnetic polarity; R = reversed magnetic polarity; T = transitional magnetic polarity; E = excursional magnetic polarity. From Beeson et al., 1989a.

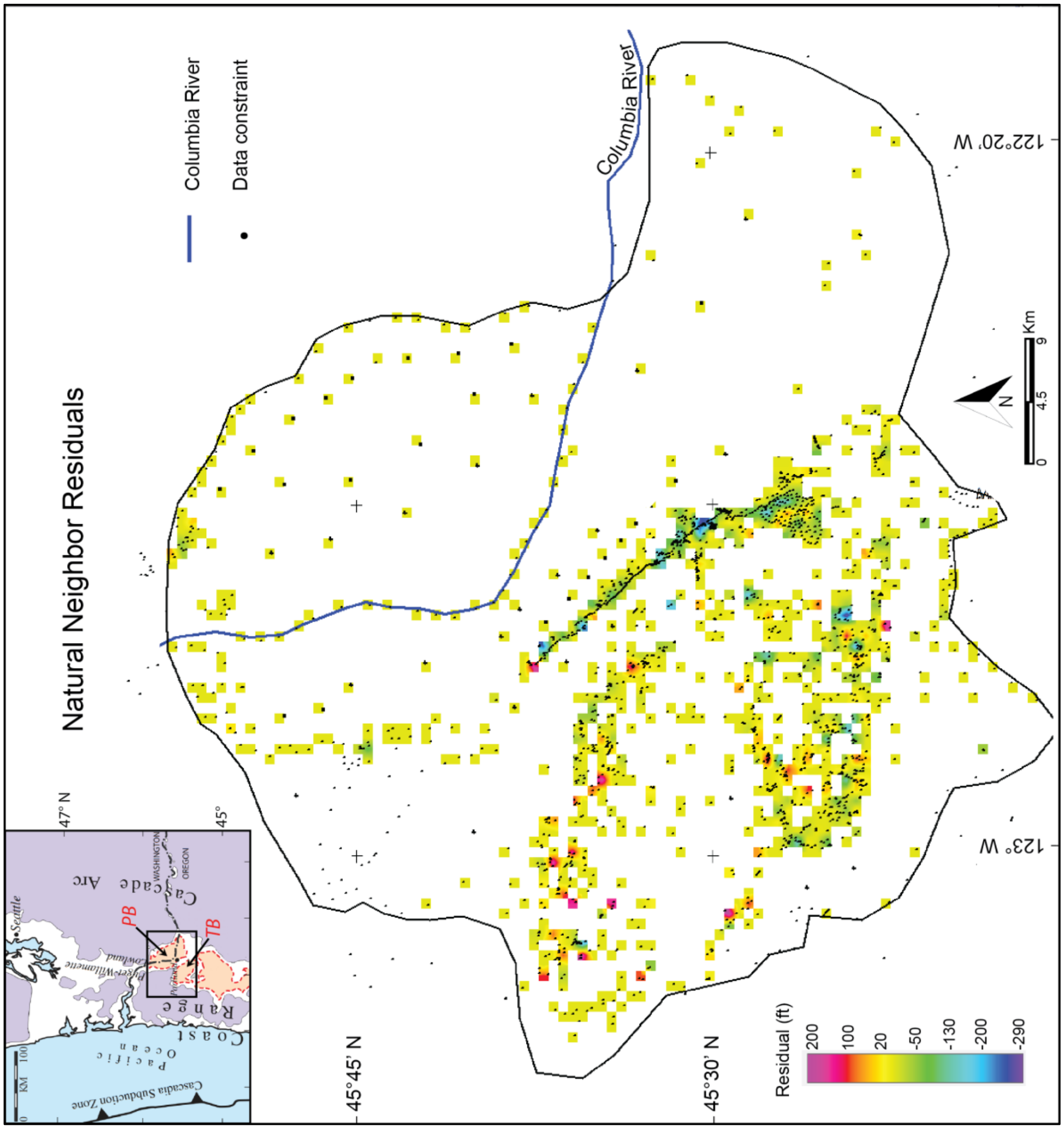

Figure A2. Residual values after subtracting top CRBG picks from interpolated values generated using the Natural Neighbor method. Residual values are positive if the data lies above the interpolated surface and negative if it lies below (Burns et al., 2011). Inset: PB – Portland basin; TB – Tualatin basin.

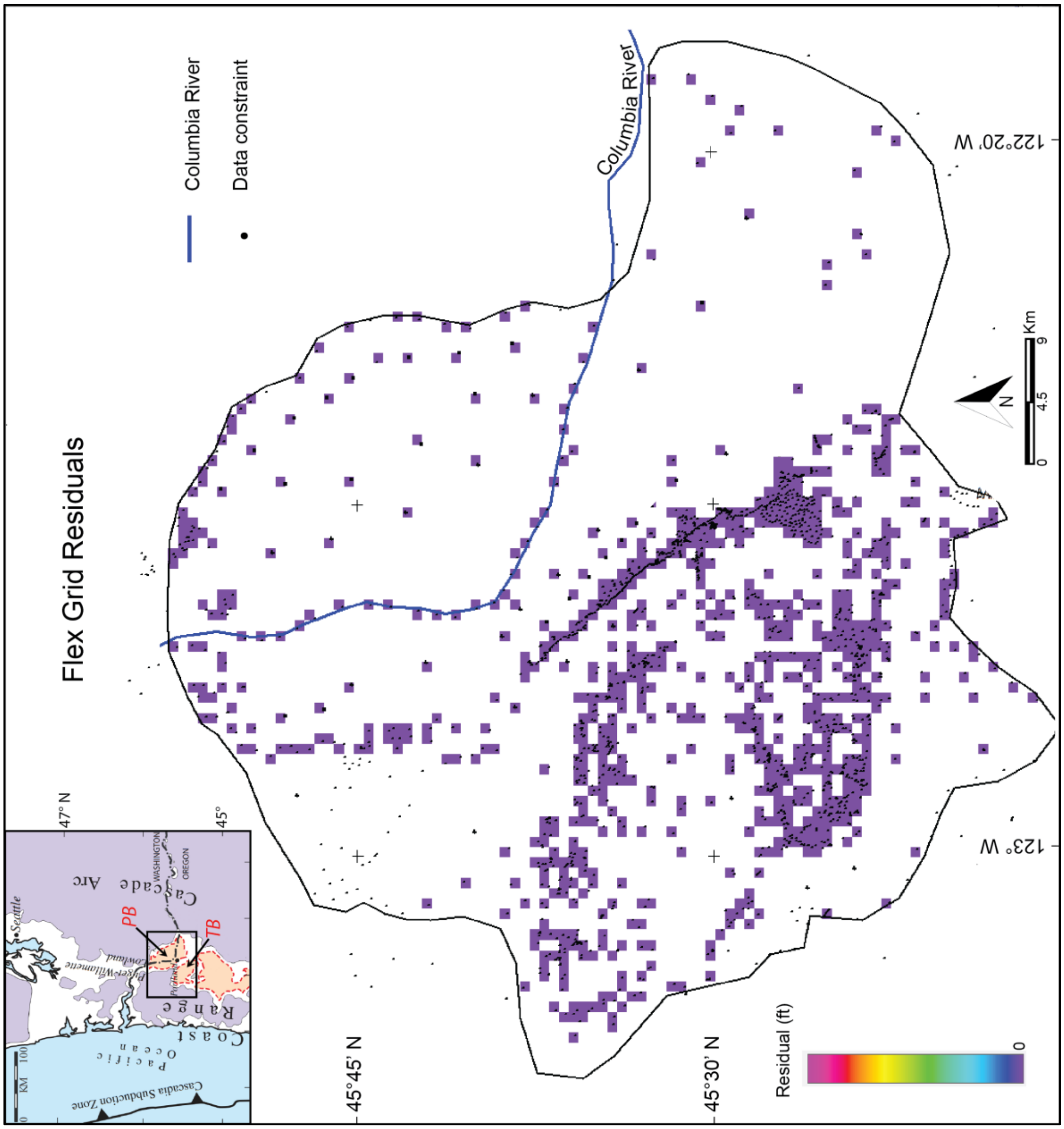

Figure A3. Residual values after subtracting top CRBG picks from interpolated values generated using the Flex Gridding method. Residual values are positive if the data lies above the interpolated surface and negative if it lies below (Burns et al., 2011). Inset: PB – Portland basin; TB – Tualatin basin.

TABLE A1: LINKS FOR PUBLICLY ACCESSIBLE DATA SOURCES USED IN THIS STUDY

Data Type	Source	URL
Water wells	Oregon Water Resources Department Groundwater Site Information System	https://apps.wrd.state.or.us/apps/gw/gw_info/gw_info_report/gw_search.aspx
	Washington Department of Natural Resources	https://www.dnr.wa.gov/geologyportal
	Washington Department of Ecology	https://fortress.wa.gov/ecy/wellconstruction/map/wclswebMap/default.aspx
Oil and Gas wells	DOGAMI Oil and Gas Well Log Index	https://www.oregongeology.org/mlrr/oilgas-logs.htm
Geologic Logs	USGS Columbia River Basalt Stratigraphy in the Pacific Northwest	https://or.water.usgs.gov/projs_dir/crbg/data/index.html
10 m DEM	USGS The National Map Database	https://viewer.nationalmap.gov/basic/

Supplemental files:

Name: “DataTable1.csv”

File type: Comma-separated values (CSV)

Size: 154 KB